Search for a very light NMSSM Higgs boson produced in decays of the 125 GeV scalar boson and decaying into τ leptons in pp collisions at $\sqrt{s} = 8$ TeV

The CMS collaboration

E-mail: cms-publication-committee-chair@cern.ch

ABSTRACT: A search for a very light Higgs boson decaying into a pair of τ leptons is presented within the framework of the next-to-minimal supersymmetric standard model. This search is based on a data set corresponding to an integrated luminosity of $19.7\,\text{fb}^{-1}$ of proton-proton collisions collected by the CMS experiment at a centre-of-mass energy of $8\,\text{TeV}$. The signal is defined by the production of either of the two lightest scalars, h_1 or h_2, via gluon-gluon fusion and subsequent decay into a pair of the lightest Higgs bosons, a_1 or h_1. The h_1 or h_2 boson is identified with the observed state at a mass of $125\,\text{GeV}$. The analysis searches for decays of the a_1 (h_1) states into pairs of τ leptons and covers a mass range for the a_1 (h_1) boson of 4 to $8\,\text{GeV}$. The search reveals no significant excess in data above standard model background expectations, and an upper limit is set on the signal production cross section times branching fraction as a function of the a_1 (h_1) boson mass. The 95% confidence level limit ranges from $4.5\,\text{pb}$ at m_{a_1} (m_{h_1}) = $8\,\text{GeV}$ to $10.3\,\text{pb}$ at m_{a_1} (m_{h_1}) = $5\,\text{GeV}$.

Contents

1 Introduction

The recently discovered particle with mass close to 125 GeV [1–3] has been shown to have properties that are consistent with those of a standard model (SM) Higgs boson [4–14]. Supersymmetric (SUSY) extensions of the SM [15, 16] also predict a particle with such properties and resolve some problems of the SM [17]. The minimal supersymmetric standard model (MSSM) [18, 19] postulates the existence of two Higgs doublets, resulting in five physical states: two CP-even, one CP-odd, and two charged Higgs bosons. This version of SUSY has been extensively tested using data collected by the ATLAS and CMS experiments at the CERN LHC. However, nonminimal SUSY extensions have received far less attention. One example is the next-to-MSSM (NMSSM), which extends the MSSM by an additional singlet superfield, interacting only with itself and the two Higgs doublets [18, 20–26]. This scenario has all the desirable features of SUSY, including a solution of the hierarchy problem and gauge coupling unification. In the NMSSM, the Higgs mixing parameter μ is naturally generated at the electroweak scale through the vacuum expectation value of the singlet field, thereby solving the so-called μ problem of the MSSM [27].

Furthermore, the amount of fine tuning required in the NMSSM to obtain a CP-even Higgs boson with a mass of 125 GeV is significantly reduced compared to the MSSM [28–30]. The Higgs sector of the NMSSM is larger than that of the MSSM. There are seven Higgs bosons: three CP-even ($h_{1,2,3}$), two CP-odd ($a_{1,2}$), and two charged Higgs states. By definition, $m_{h_3} > m_{h_2} > m_{h_1}$ and $m_{a_2} > m_{a_1}$. Over large parts of the NMSSM parameter space, the observed boson with mass close to 125 GeV, hereafter denoted H(125), could be identified with one of the two lightest scalar NMSSM Higgs bosons, h_1 or h_2.

A vast set of next-to-minimal supersymmetric models is consistent with the SM measurements and constraints from searches for SUSY particles made with LHC, Tevatron, SLAC and LEP data, as well as with the properties of the H(125) boson measured using Run 1 LHC data [31–36]. These models provide possible signatures that cannot be realized in the MSSM given recent experimental constraints [37]. For example, the decays H(125) $\rightarrow$ h$_1$h$_1$ and H(125) $\rightarrow$ a$_1$a$_1$ are allowed when kinematically possible. These decay signatures have been investigated in phenomenological studies considering a variety of production modes at the LHC [38–45]. The analysis presented in this paper is motivated by the NMSSM scenarios that predict a very light h$_1$ or a$_1$ state with mass in the range $2m_\tau < m_{h_1}\ (m_{a_1}) < 2m_b$, where m_τ is the mass of the τ lepton and m_b is the mass of the b quark. Such a light state is potentially accessible in final states with four τ leptons, where H(125) $\rightarrow$ h$_1$h$_1$ (a$_1$a$_1$) $\rightarrow 4\tau$ [46, 47]. In these scenarios the decay H(125) $\rightarrow$ a$_2$a$_2$ is not kinematically allowed.

Several searches for H(125) $\rightarrow \phi_1\phi_1$ decays, where ϕ_1 can be either the lightest CP-even state h$_1$ or the lightest CP-odd state a$_1$, have been performed. The analyses carried out by the OPAL and ALEPH Collaborations at LEP [48, 49] searched for the decay of the CP-even Higgs boson into a pair of light CP-odd Higgs bosons, exploiting the Higgs-strahlung process, where the CP-even state is produced in association with a Z boson. These searches found no evidence for a signal, and limits were placed on the signal production cross section times branching fraction. However, searches at LEP did not probe masses of the CP-even state above 114 GeV. A similar study has been performed by the D0 Collaboration at the Tevatron [50], searching for inclusive production of the CP-even Higgs boson in p$\overline{\text{p}}$ collisions followed by its decay into a pair of light CP-odd Higgs bosons. No signal was detected and upper limits were set on the signal production cross section times branching fraction in the mass ranges $3.6 < m_{a_1} < 19$ GeV and $89 < m_H < 200$ GeV. The limits set by the D0 analysis are a factor one to seven times higher compared to the SM production cross section for p$\overline{\text{p}} \rightarrow$ H(125) + X.

The CMS Collaboration has recently searched for a very light CP-odd Higgs boson produced in decays of a heavier CP-even state [51]. This study probed the mass of the CP-odd state in the range $2m_\mu < m_{a_1} < 2m_\tau$, where m_μ is the mass of muon. In this mass range the decay a$_1 \rightarrow \mu\mu$ can be significant. No evidence for a signal was found and upper limits were placed on the signal production cross section times branching fraction. The ATLAS Collaboration has also recently searched for h/H $\rightarrow$ a$_1$a$_1 \rightarrow \mu\mu\tau\tau$ [52], covering the mass range $m_{a_1} = 3.7$–50 GeV for $m_H = 125$ GeV, and $m_H = 100$–500 GeV for $m_{a_1} = 5$ GeV. No excess over SM backgrounds was observed, and upper limits were placed on

$\sigma(\text{gg} \to \text{H}) \, \mathcal{B}(\text{H} \to \text{a}_1 \text{a}_1) \, \mathcal{B}^2(\text{a}_1 \to \tau\tau)$, under the assumption that

$$\frac{\Gamma(\text{a} \to \mu\mu)}{\Gamma(\text{a} \to \tau\tau)} = \frac{m_\mu^2}{m_\tau^2 \sqrt{1 - \left(2m_\tau/m_\text{a}\right)^2}}.$$

The search for the production of a pair of light bosons with their subsequent decay into four τ leptons has not yet been performed at the LHC and is the subject of this paper. The choice of the 4τ channel makes it possible to probe the signal cross section times branching fraction

$$(\sigma\mathcal{B})_\text{sig} \equiv \sigma(\text{gg} \to \text{H}(125)) \, \mathcal{B}(\text{H}(125) \to \phi_1\phi_1) \, \mathcal{B}^2(\phi_1 \to \tau\tau)$$

in a model-independent way.

2 Signal topology

This paper describes a search for the production of the H(125) boson, with its decay into a pair of light NMSSM Higgs bosons ϕ_1. The signal can be associated with one of three possible scenarios:

- H(125) corresponds to h_2 and decays into a pair of h_1 states, $\text{h}_2 \to \text{h}_1\text{h}_1$;

- H(125) corresponds to h_2 and decays into a pair of a_1 states, $\text{h}_2 \to \text{a}_1\text{a}_1$;

- H(125) corresponds to h_1 and decays into a pair of a_1 states, $\text{h}_1 \to \text{a}_1\text{a}_1$.

The analysis is optimized for the gluon-gluon fusion process, which is the dominant production mechanism of the H(125) boson at the LHC. The signal topology is illustrated in figure 1. The search is performed for very light ϕ_1 states, covering a mass range of 4 to 8 GeV. Within this mass range the ϕ_1 boson is expected to decay predominantly into a pair of τ leptons, $\phi_1 \to \tau\tau$. In the decay of each ϕ_1, one of the τ leptons is identified via its muonic decay. The other τ lepton is required to decay into a one-prong mode, i.e. a decay into one charged particle (electron, muon, or hadron) and one or more neutral particles. We identify these decays by the presence of one reconstructed track with charge sign opposite to that of the closest muon. Neutral particles are not considered in the event selection.

Given the large difference in mass between the ϕ_1 and the H(125) states ($m_{\text{H}(125)} \gg m_{\phi_1}$), one expects the ϕ_1 bosons to have large Lorentz boosts and their decay products to be collimated. Furthermore, in the gluon-gluon fusion process the H(125) state is mainly produced with relatively small transverse momentum p_T. Thus, in the majority of H(125) $\to \phi_1\phi_1$ decays, the ϕ_1 states would be produced nearly back-to-back in the plane transverse to the beams, with a large separation in azimuthal angle ϕ between the decay products of the two ϕ_1 bosons. The H(125) state can be produced with relatively high transverse momentum if a hard gluon is radiated from the initial-state gluons or the heavy-quark loop. In this case, the separation between two ϕ_1 bosons in azimuthal angle is reduced, while the separation in pseudorapidity η can still be large. The pseudorapidity is defined via the polar angle θ as $\eta \equiv -\ln\left[\tan\left(\theta/2\right)\right]$.
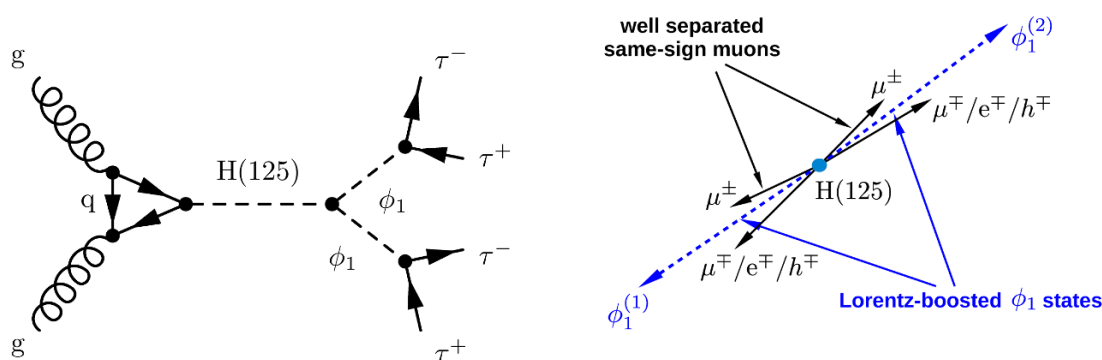
Figure 1. Left: Feynman diagram for the signal process. Right: illustration of the signal topology. The label "$\mu^{\mp}/\mathrm{e}^{\mp}/h^{\mp}$" denotes a muon, electron, or charged-hadron track.

The $\phi_1 \to \tau\tau$ decays into final states without muons are not considered in the analysis. These decays are mimicked by hadronic jets with a significantly higher probability compared to final states with at least one muon and contribute marginally to the search sensitivity.

The signal properties discussed above are used to define the search topology. The analysis presented here searches for the signal in a sample of dimuon events with large angular separation between the muons. The two muons are required to have the same sign. This criterion almost entirely eliminates background from the Drell-Yan process, gauge boson pair production, and $t\bar{t}$ production. Each muon is accompanied by one nearby opposite-sign track. Further details of the kinematic selection are given in section 4. Throughout this paper, the signal yields are normalized to the benchmark value of the signal production cross section times branching fraction of 5 pb. The choice of the benchmark scenario is motivated by recent phenomenological analyses [46, 47].

3 CMS detector, data, and simulated samples

The central feature of the CMS apparatus is a superconducting solenoid of 6 m internal diameter, providing a field of 3.8 T. The innermost component of the detector is a silicon pixel and strip tracker, which is used to measure the momenta of charged particles and reconstruct collision vertices. The tracker, which covers the pseudorapidity range $|\eta| < 2.5$, is surrounded by a crystal electromagnetic calorimeter and a brass and scintillator hadronic calorimeter, both placed inside the solenoid. These calorimeters cover $|\eta| < 3.0$. A quartz fiber Cherenkov forward hadron detector extends the calorimetric coverage to $|\eta| < 5.0$. Muons are measured in the pseudorapidity range $|\eta| < 2.4$, with detection planes made using three technologies: drift tubes, cathode strip chambers, and resistive-plate chambers. The first level of the CMS trigger system, composed of custom hardware processors, uses information from the calorimeters and muon detectors to select the most interesting events in a fixed time interval of $4\,\mu$s. The high-level trigger processor farm further decreases the event rate from around 100 kHz to less than 1 kHz before data storage. A more detailed

description of the CMS detector, together with a definition of the coordinate system used and the relevant kinematic variables, can be found in ref. [53].

The data set used in this analysis was recorded in 2012 and corresponds to an integrated luminosity of $19.7\,\mathrm{fb}^{-1}$ of pp collisions at $\sqrt{s} = 8\,\mathrm{TeV}$.

The Monte Carlo (MC) event generator PYTHIA 6.426 [54] is used to model the NMSSM Higgs boson signal produced via gluon-gluon fusion. The H(125) boson p_T spectrum from PYTHIA is reweighted to the spectrum obtained from a next-to-leading-order computation with a next-to-next-to-leading logarithmic accuracy using the HQT 2.0 program [55, 56], which performs the resummation of the large logarithmic contributions appearing at transverse momenta much smaller than the mass of the Higgs boson. For optimisation studies, diboson and quantum chromodynamics (QCD) multijet backgrounds are simulated by PYTHIA. Inclusive Z, W, and $t\bar{t}$ production are modelled with MADGRAPH 5.1 [57]. The MADGRAPH generator is interfaced with PYTHIA for parton showering and fragmentation. The PYTHIA parameters that steer the simulation of hadronisation and the underlying event are set to the most recent PYTHIA Z2* tune. This tune is derived from the Z1 tune [58], which uses the CTEQ5L parton distribution function (PDF) set, whereas Z2* adopts the CTEQ6L PDF set [59]. The TAUOLA package [60] is used for τ lepton decays in all cases. All generated events, with the exception of a few special QCD multijet samples discussed in section 6.2, are processed through a detailed simulation of the CMS detector, based on GEANT4 [61], and are reconstructed employing the same algorithms as for data.

4 Event selection

Events are recorded using double-muon triggers with thresholds on the muon transverse momenta of 17 GeV for the leading muon and 8 GeV for the subleading one. To pass the high-level trigger, the tracks of the two muons are additionally required to have points of closest approach to the beam axis within 2 mm of each other along the longitudinal direction.

In 2012, the average number of pp interactions per LHC bunch crossing (pileup) was about 20. The simulated MC events are reweighted to represent the distribution of the number of pileup interactions per bunch crossing in data.

For each reconstructed collision vertex, the sum of the p_T^2 of all tracks associated with the vertex is computed. The vertex for which this quantity is largest is assumed to correspond to the hard-scattering process, and is referred to as the primary vertex (PV).

The identification and reconstruction of muons is achieved by matching track segments found in the silicon tracker with those found in the muon detectors [62]. Additional requirements are applied on the number of measurements in the inner pixel and outer silicon strip detectors, on the number of matched segments in the muon detectors, and on the quality of the global muon track fit, quantified by χ^2.

The data are further selected by requiring at least one pair of muons with the same charge. This requirement significantly suppresses background contributions originating from the Drell-Yan process, from decays of $t\bar{t}$ pairs, and from QCD multijet events with muonic decays of heavy-flavour hadrons. The leading muon is required to have $p_\mathrm{T} > 17\,\mathrm{GeV}$ and $|\eta| < 2.1$. The subleading muon is required to have $p_\mathrm{T} > 10\,\mathrm{GeV}$ and $|\eta| < 2.1$. To

reject QCD multijet events with muonic decays of hadrons containing charm or bottom quarks, selections are applied on the impact parameters of the muon tracks. The impact parameter in the transverse plane is required to be smaller than $300\,\mu$m with respect to the PV. The longitudinal impact parameter is required to be smaller than $1\,$mm with respect to the PV. The two selected same-sign muons are required to be separated by $\Delta R(\mu, \mu) = \sqrt{\Delta\eta^2 + \Delta\phi^2} > 2$, where $\Delta\eta$ is the separation in pseudorapidity and $\Delta\phi$ is the separation in azimuthal angle between the two muons. If more than one same-sign muon pair is found in the event, the pair with the largest scalar sum of muon transverse momenta is chosen.

The analysis makes use of reconstructed tracks that fulfill selection criteria based on the track fit quality, the number of measurements in the inner pixel and outer strip silicon detector, and track impact parameters with respect to the PV [63]. Tracks must have $p_{\mathrm{T}} > 1\,$GeV and $|\eta| < 2.4$. The impact parameter in the transverse plane and the longitudinal impact parameter are required to be smaller than $1\,$cm relative to the PV.

Given the search topology, we require each muon to be accompanied by exactly one track satisfying these criteria within a ΔR cone of radius 0.5 centred on the muon direction. We label such muon-track pairs as "isolated".

The loose impact parameter requirements on the tracks are designed to suppress background events in which a heavy-flavour hadron decays into a muon and several charged particles. Although tracks from these decay products will be displaced from the PV, they can still satisfy the loose track impact parameter criteria. Such events are rejected by the requirement of exactly one track accompanying the muon.

The track around each muon is identified as a one-prong τ lepton decay candidate if it fulfils the following selection criteria.

- The nearby track is required to have charge opposite to the muon.

- The track must have $p_{\mathrm{T}} > 2.5\,$GeV and $|\eta| < 2.4$.

- The transverse and longitudinal impact parameters of the track are required to be smaller than $200\,\mu$m and $400\,\mu$m relative to the PV, respectively.

5   Signal extraction

The set of selection requirements outlined in the previous section defines the signal region. The number of selected data events, the expected background and signal yields, and the signal acceptances after selection in the signal region are reported in table 1. The expected background and signal yields, along with the signal acceptances, are obtained from simulation. The signal yields are normalized to the benchmark value of the signal production cross section times branching fraction of $5\,$pb. The quoted uncertainties in predictions from simulation include only MC statistical uncertainties. It should be noted that no MC simulation is used to evaluate the background in the analysis described below as the modelling is based fully on data. The expected background yields presented in table 1 show that the final selected sample is dominated by QCD multijet events, and that the

contribution from other background sources is negligible, constituting less than 1% of all selected events. Although MC simulation is not directly used to estimate background, the simulated samples play an important role in the validation of the background modelling as described in section 6. The signal acceptances are computed with respect to all possible decays of the four τ leptons, and include a branching fraction factor

$$\frac{1}{2}\mathcal{B}^2(\phi_1 \to \tau_\mu\tau_{\text{one-prong}}) \approx 3.5\%,$$

where the factor $1/2$ accounts for the selection of same-sign muon pairs, and $\mathcal{B}(\phi_1 \to \tau_\mu\tau_{\text{one-prong}})$ denotes the branching fraction of the $\phi_1 \to \tau\tau$ decays to the final states characterized by the presence of only two charged particles where at least one of the charged particles is a muon. This branching fraction is expressed as

$$\mathcal{B}(\phi_1 \to \tau_\mu\tau_{\text{one-prong}}) = 2\mathcal{B}(\tau \to \text{one-prong})\mathcal{B}(\tau \to \mu\nu\overline{\nu}) - \mathcal{B}^2(\tau \to \mu\nu\overline{\nu}),$$

where $\mathcal{B}(\tau \to \text{one-prong})$ denotes the total branching fraction of the τ decay to one charged particle with any number of neutral particles. The factor of two in the first term accounts for the two possible charges of the required muonic decay: $\tau^-\tau^+ \to \mu^- + \text{one-prong}^+$ and $\tau^-\tau^+ \to \mu^+ + \text{one-prong}^-$. Subtraction of the term $\mathcal{B}^2(\tau \to \mu\nu\overline{\nu})$ avoids double counting in the case where the two τ leptons produced by a given ϕ_1 both decay to muons.

The invariant mass of each selected muon and the nearby track is reconstructed. The two-dimensional distribution of the invariant mass of each selected muon and the nearby track is used to discriminate between the signal and the QCD multijet background; the signal is extracted by means of a fit to this two-dimensional distribution. The binning of the two-dimensional (m_1, m_2) distributions is illustrated in figure 2. For masses below $3\,\text{GeV}$, bins of $1\,\text{GeV}$ width are used for both m_1 and m_2. For masses in the range $3 < m_1(m_2) < 10\,\text{GeV}$, a single bin is used. This choice avoids poorly populated bins in the two-dimensional (m_1, m_2) distributions in the background control regions used to construct and validate the QCD multijet background model (section 6). For each selected event, the (m_1, m_2) histogram is filled once if the pair of quantities (m_1, m_2) occurs in one of the diagonal bins and twice, once with values (m_1, m_2) and a second time with the swapped values (m_2, m_1), for off-diagonal bins. This procedure insures the symmetry of the two-dimensional (m_1, m_2) distribution. To avoid double counting of events, the off-diagonal bins (i, j) with $i > j$ are excluded from the procedure of the signal extraction (the hatched bins in figure 2). Thus, the number of independent bins is reduced from $4 \times 4 = 16$ to $4 \times (4 + 1)/2 = 10$.

In order to fit the data in the 10 bins of the two-dimensional distribution of figure 2, a two-component fit is performed using two-dimensional distributions ("templates") describing the QCD multijet background and the signal. The normalisations of background and signal components are free parameters in this fit. The two-dimensional template for the signal is obtained from the simulation using the generator described in section 3. The two-dimensional template for the QCD multijet background is extracted from the data as explained in the next section.

Sample	Signal acceptance $\mathcal{A}(\text{gg} \to \text{H}(125) \to \phi_1\phi_1 \to 4\tau)$	Number of events
Signal		for $(\sigma\mathcal{B})_{\text{sig}} = 5\,\text{pb}$
$\quad m_{\phi_1} = 4\,\text{GeV}$	$(5.38 \pm 0.23) \times 10^{-4}$	53.0 ± 2.3
$\quad m_{\phi_1} = 5\,\text{GeV}$	$(4.36 \pm 0.21) \times 10^{-4}$	43.0 ± 2.0
$\quad m_{\phi_1} = 6\,\text{GeV}$	$(4.00 \pm 0.23) \times 10^{-4}$	39.5 ± 2.0
$\quad m_{\phi_1} = 7\,\text{GeV}$	$(4.04 \pm 0.20) \times 10^{-4}$	39.9 ± 2.0
$\quad m_{\phi_1} = 8\,\text{GeV}$	$(3.13 \pm 0.18) \times 10^{-4}$	30.8 ± 1.8
Background		
$\quad$ QCD multijet	—	820 ± 320
$\quad$ t$\bar{\text{t}}$	—	1.2 ± 0.2
$\quad$ Electroweak	—	5.0 ± 4.7
Data	—	873

Table 1. The number of observed events, expected background and signal yields, and signal acceptances after final selection. The computed signal acceptances include the branching fraction factor $\mathcal{B}^2(\phi_1 \to \tau_\mu\tau_{\text{one-prong}})/2$. The electroweak background contribution includes the Drell-Yan process, W + jets production, and diboson production of WW, WZ, and ZZ. The numbers of signal events are reported for the benchmark value of the signal production cross section times branching fraction of 5 pb. The expected background and signal yields and signal acceptances are obtained from simulation. The quoted uncertainties in predictions from simulation include only statistical uncertainties related to the size of MC samples.

6 Modelling of the QCD multijet background shape

A simulation study shows that the sample of same-sign dimuon events selected as described in section 4, but without requiring a presence of one-prong τ candidates and without applying the isolation requirement for the muon-track systems, is dominated by QCD multiparton production, where 94% of all selected events contain b quarks in the final state. The same-sign muon pairs in these events originate mainly in the following cases.

- Muonic decay of a bottom hadron in one b quark jet, and cascade decay of a bottom hadron into a charmed hadron with subsequent muonic decay of a charmed hadron in the other b quark jet.

- Muonic decay of a bottom hadron in one b quark jet, and decay of a quarkonium state into a pair of muons in the other jet.

- Muonic decay of a bottom hadron in one b quark jet, and muonic decay of a neutral B meson in the other b quark jet. The same-sign muon pair in this case may appear as a result of B^0–$\overline{\text{B}}^0$ oscillations.
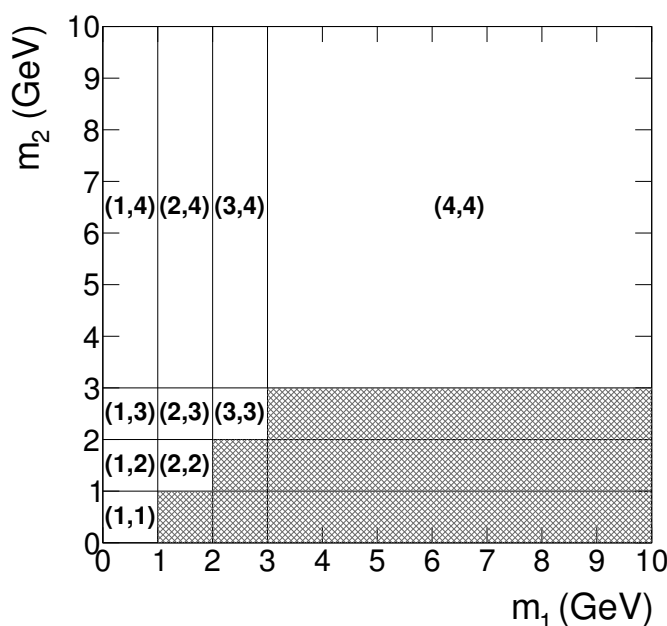
Figure 2. Binning of the two-dimensional (m_1, m_2) distribution. The hatched bins are excluded from the statistical analysis, as detailed in the text.

The normalization of the QCD multijet background is not constrained prior to the extraction of the signal. The procedure used to model the shape of the two-dimensional (m_1, m_2) distribution of QCD multijet events in the signal region is described in this section.

Given the symmetry of the two-dimensional (m_1, m_2) distribution, the modelling of the QCD multijet background shape is derived from the two-dimensional probability density function (pdf)

$$f_{2D}(m_1, m_2) = C(m_1, m_2) f_{1D}(m_1) f_{1D}(m_2), \tag{6.1}$$

where

- $f_{2D}(m_1, m_2)$ is the two-dimensional pdf of the invariant masses of the muon-track systems, m_1 and m_2, in the sample of QCD multijet events selected in the signal region;

- $f_{1D}(m_i)$ is the one-dimensional pdf of the invariant mass of the muon-track system in the sample of QCD multijet events selected in the signal region;

- $C(m_1, m_2)$ is a symmetric function of two arguments, $C(m_1, m_2) = C(m_2, m_1)$, reflecting the correlation between m_1 and m_2.

A constant correlation function would indicate the absence of correlation between m_1 and m_2. Based on eq. (6.1), the content of bin (i, j) of the symmetric normalized two-dimensional distribution $f_{2D}(m_1, m_2)$ is computed as

$$f_{2D}(i, j) = C(i, j) f_{1D}(i) f_{1D}(j), \tag{6.2}$$

where

- $C(i, j)$ is the correlation coefficient in the bin (i, j) of the correlation function $C(m_1, m_2)$;

- $f_{1D}(i)$ is the content of bin i in the normalized one-dimensional distribution $f_{1D}(m)$.

The modelling of $f_{1D}(m)$ and $C(m_1, m_2)$, described in the following, is necessary in order to build the template $f_{2D}(i, j)$.

6.1 Modelling of $f_{1D}(m)$

The $f_{1D}(m)$ pdf is modelled using a QCD-enriched control data sample disjoint from the signal region. Events in the control sample are required to satisfy all selection criteria, except for the isolation of the second muon-track system. The second muon is required to be accompanied by either two or three nearby tracks with $p_T > 1\,\text{GeV}$ and impact parameters smaller than $1\,\text{cm}$ relative to the PV both in the transverse plane and along the beam axis. The simulation shows that more than 99% of events selected in this control region, hereafter referred to as $\mathbf{N_{23}}$, are QCD multijet events. The modelling of the $f_{1D}(m)$ pdf is based on the assumption that the kinematic distributions for the first muon-track system are not affected by the isolation requirement imposed on the second, and therefore the $f_{1D}(m)$ pdf of the isolated muon-track system is the same in the signal region and the region $\mathbf{N_{23}}$.

A direct test of this assumption, given the limited size of the simulated sample of QCD multijet events, is not conclusive, and a test is therefore performed with an additional control sample. Events are selected in this control sample if one of the muons has at least one track passing the one-prong τ decay candidate criteria within a ΔR cone of radius 0.5 around the muon direction, with any number of additional tracks within the same ΔR cone. As more than one of these tracks can pass the selection criteria for a one-prong τ decay candidate, we investigate two scenarios. In one scenario, the lowest p_T ("softest") track passing the one-prong τ decay candidate criteria is used to calculate the muon-track invariant mass, while in the other scenario the highest p_T ("hardest") track passing the one-prong τ decay candidate criteria is used. If only one τ track is found around the first muon, the track is regarded as both "hardest" and "softest". For the second muon, two isolation requirements are considered: when the muon is accompanied by only one track passing the one-prong τ decay candidate criteria ($N_{\text{trk},2} = 1$) as in the signal region, or when it is accompanied by two or three tracks ($N_{\text{trk},2} = 2, 3$) with $p_T > 1\,\text{GeV}$ and impact parameters smaller than $1\,\text{cm}$ relative to the PV as in the region $\mathbf{N_{23}}$. The shapes of invariant mass distributions of the first muon and the softest or hardest accompanying track are then compared for the two different isolation requirements on the second muon, $N_{\text{trk},2} = 1$ and $N_{\text{trk},2} = 2, 3$. The test is performed both on data and on the simulated sample of QCD multijet events. The results of this study are illustrated in figure 3. In all considered cases, the shape of the invariant mass distribution is compatible within statistical uncertainties between the two cases, $N_{\text{trk},2} = 1$ and $N_{\text{trk},2} = 2, 3$. This observation validates the assumption that the $f_{1D}(m)$ pdf can be determined in the control region $\mathbf{N_{23}}$.
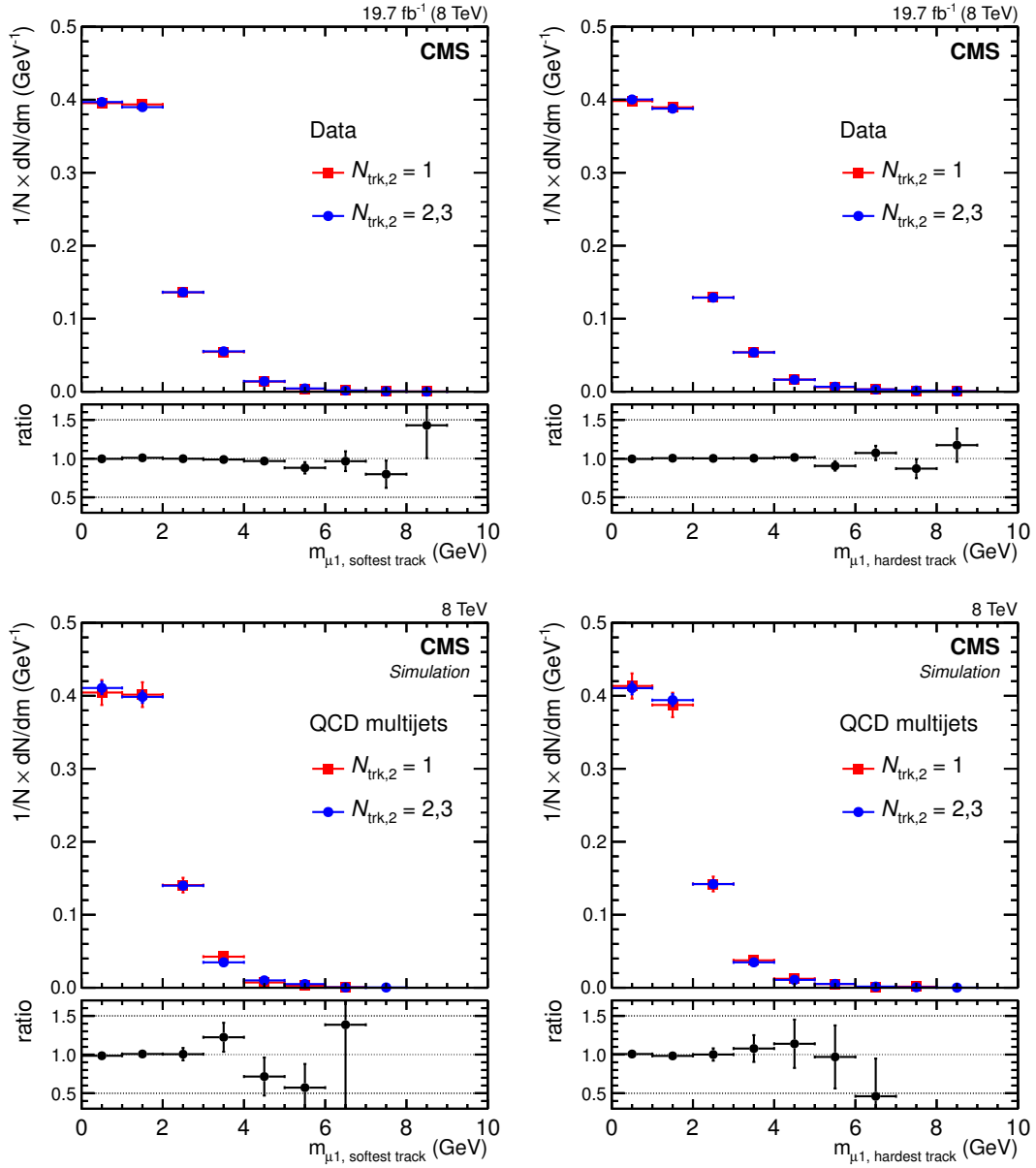
Figure 3. Normalized invariant mass distributions of the first muon and the softest (left plots) or hardest (right plots) accompanying track for different isolation requirements imposed on the second muon: when the second muon has only one accompanying track ($N_{\mathrm{trk},2} = 1$; squares); or when the second muon has two or three accompanying tracks ($N_{\mathrm{trk},2} = 2, 3$; circles). The upper plots show distributions obtained from data. The lower plots show distributions obtained from the sample of QCD multijet events generated with PYTHIA. Lower panels in each plot show the ratio of the $N_{\mathrm{trk},2} = 1$ distribution to the $N_{\mathrm{trk},2} = 2, 3$ distribution.

Figure 4 presents the normalized invariant mass distribution of the muon-track system for data selected in the signal region, and for the QCD multijet background model derived from the control region $\mathbf{N}_{23}$. The data and QCD multijet background distributions are compared to the signal distribution normalized to unity (signal pdf), obtained from sim-
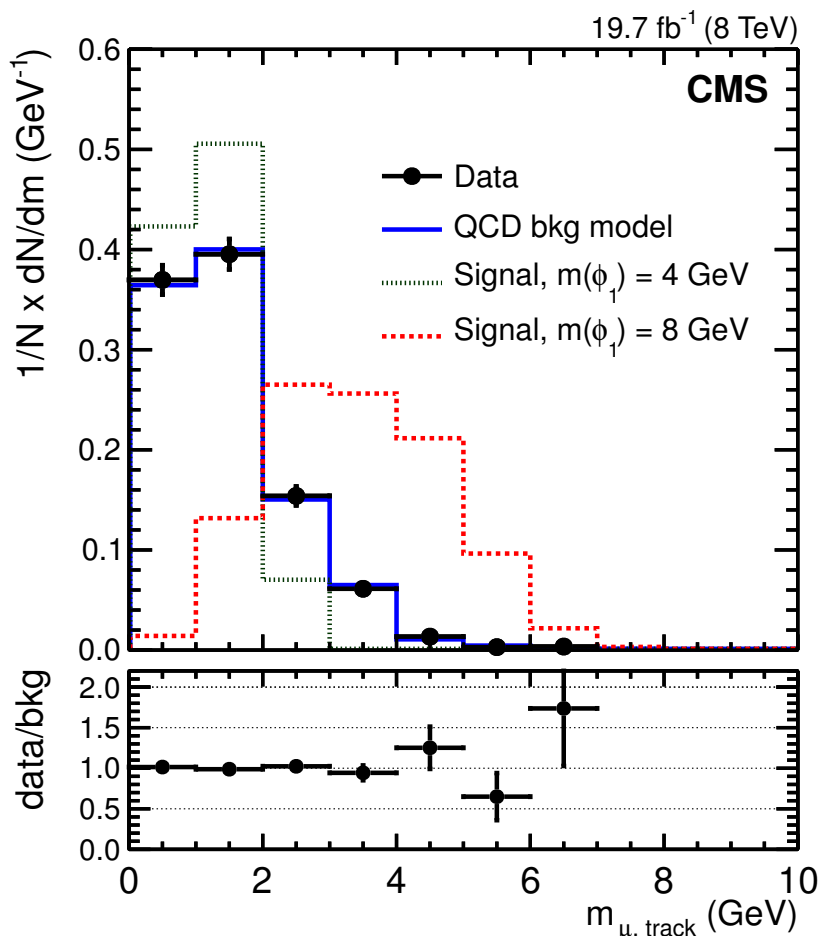
Figure 4. Normalized invariant mass distribution of the muon-track system for events passing the signal selection. Data are represented by points. The QCD multijet background model is derived from the control region $\mathbf{N}_{23}$. Also shown are the normalized distributions from signal simulations for two mass hypotheses, $m_{\phi_1} = 4\,\text{GeV}$ (dotted histogram) and $8\,\text{GeV}$ (dashed histogram). Each event contributes two entries to the distribution, corresponding to the two muon-track systems passing the selection requirements. The lower panel shows the ratio of the distribution observed in data to the distribution, describing the background model.

ulation, for two representative mass hypotheses, $m_{\phi_1} = 4$ and $8\,\text{GeV}$. The invariant mass of the muon-track system is found to have high discrimination power between the QCD multijet background and signal at $m_{\phi_1} = 8\,\text{GeV}$. At smaller m_{ϕ_1} the signal shape becomes more similar to the background shape, resulting in a reduction of discrimination power. The normalized distribution $f_{1D}(i)$ with the binning defined in figure 2 is extracted from the background distribution shown in figure 4.

6.2 Modelling of $C(m_1, m_2)$

In order to determine the correlation coefficients $C(i, j)$ we define an additional control region $\mathbf{A}$ enriched in QCD multijet events. This control region consists of events that contain two same-sign muons passing the identification and kinematic selection criteria
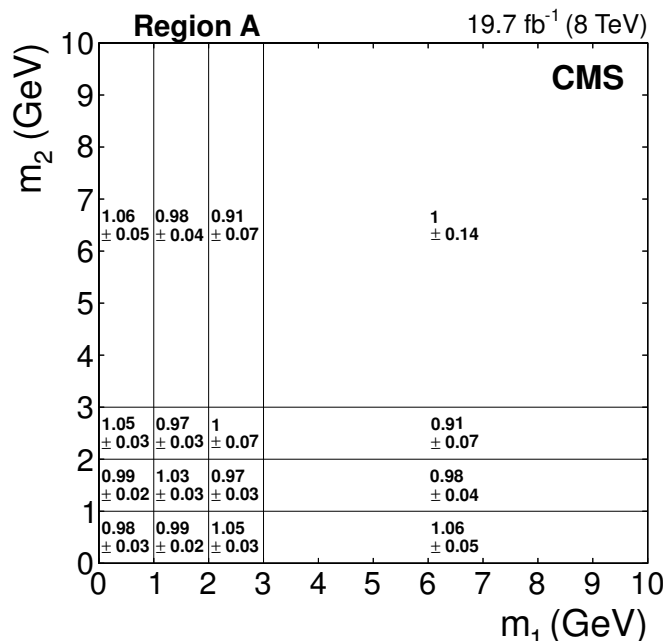
Figure 5. The (m_1, m_2) correlation coefficients $C(i,j)$ along with their statistical uncertainties, derived from data in the control region **A**.

outlined in section 4. Each muon is required to have two or three nearby tracks within a ΔR cone of radius 0.5 around the muon direction. One and only one of these tracks must satisfy the criteria imposed on one-prong τ lepton decay candidates with $p_T > 2.5$ GeV. The additional tracks must have transverse momentum in the range $1 < p_T < 2.5$ GeV. A total of 9127 data events are selected in this control region. The MC simulation predicts that the QCD multijet background dominates in region **A**, comprising more than 99% of all selected events. The simulation study also shows that the overall background-to-signal ratio is enhanced compared to the signal region by a factor of 15 to 20, depending on the mass hypothesis m_{ϕ_1}. Despite the large increase in the overall background-to-signal ratio, potential signal contamination in individual bins of the mass distributions can be nonnegligible. Bin-by-bin signal contamination in region **A** is discussed in section 7. For each event in control region **A**, the pair (m_1, m_2) of muon-track invariant masses is calculated. This pair is used to build the symmetrized normalized two-dimensional distribution $f_{2D}(i,j)$ defined in figure 2. Then $C(i,j)$ is obtained according to eq. (6.2) as

$$C(i,j) = \frac{f_{2D}(i,j)}{f_{1D}(i)\, f_{1D}(j)}, \tag{6.3}$$

where $f_{1D}(i)$ is the one-dimensional normalized distribution with two entries per event (m_1 and m_2) built as for figure 4. Correlation coefficients $C(i,j)$ derived from data in region **A** are presented in figure 5.

A direct comparison of $C(i,j)$ between the signal region and region **A** would be impossible in the simulated sample of QCD multijet events because of the very small numbers of events selected in the signal region and in region **A**. In order to assess the difference

in $C(i,j)$ between the signal region and region **A**, a dedicated MC study is performed, making use of a large exclusive sample generated with PYTHIA. The simulation includes only two leading-order QCD multijet production mechanisms: the creation of a $b\overline{b}$ quark pair via gg $\to$ $b\overline{b}$ and $q\overline{q} \to b\overline{b}$. The detector simulation and event reconstruction are not performed for this sample, and the comparison of $C(i,j)$ between the signal region and region **A** is made using generator-level quantities.

These simplifications are validated by performing a set of consistency tests, making use of the available MC sample of QCD multijet events processed through the full detector simulation and event reconstruction. These tests are performed in a control region **B**, where each muon is required to have at least one track passing the one-prong τ decay candidate selection criteria, i.e. with $p_T > 2.5\,\text{GeV}$ and impact parameters smaller than $200\,\mu\text{m}$ and $400\,\mu\text{m}$ in the transverse plane and along beam axis, respectively. Along with this requirement each muon is allowed to have one or more tracks within a ΔR cone of radius 0.5 around the muon direction, with $p_T > 1\,\text{GeV}$ and impact parameters smaller than 1 cm. Control region **B** is characterized by a significantly larger yield of QCD multijet events compared to the signal region and control region **A**, thus making it possible to perform reliable MC consistency tests and assess the uncertainties in $C(i,j)$. Two scenarios are investigated: 1) muons are paired with the softest one-prong τ decay candidate and 2) muons are paired with the hardest one-prong τ decay candidate. If only one one-prong τ decay candidate is found around a muon, it is regarded as both "softest" and "hardest". In both scenarios the correlation coefficients computed using the reconstructed four-momenta of muons and tracks are found to be compatible with those computed using generator-level four-momenta, within statistical uncertainties. Furthermore, the correlation coefficients computed with the inclusive QCD multijet sample are found to be compatible with those computed in the exclusive MC sample including only the gg($q\overline{q}$) $\to$ $b\overline{b}$ production mechanisms. This observation validates the use of the generator-level information and the exclusive $b\overline{b}$ MC sample to compare $C(i,j)$ between the signal region and control region **A**. This comparison is presented in figure 6. The uncertainties in $C(i,j)$ represent a quadratic sum of the systematic and MC statistical uncertainties. The systematic uncertainties are derived from the control region **B**. They take into account 1) any differences in $C(i,j)$ calculated using the inclusive QCD multijet sample compared with the exclusive $b\overline{b}$ sample and 2) any differences in $C(i,j)$ calculated using full detector simulation and event reconstruction compared with the study using generator-level quantities. Within their uncertainties the correlation coefficients $C(i,j)$ in the signal region and in region **A** are compatible. We therefore use $C(i,j)$ derived from data in region **A** to predict the QCD multijet background shape in the signal region according to eq. (6.2).

7 Systematic uncertainties

The analysis is affected by various systematic uncertainties, which are classified into two groups. The first group consists of uncertainties related to the background, while the second group includes uncertainties related to the signal. The systematic uncertainties are summarized in table 2.
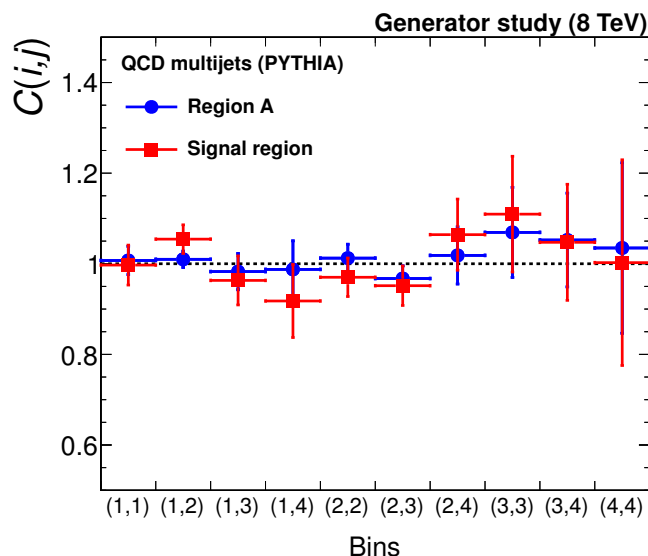
Figure 6. The (m_1, m_2) correlation coefficients $C(i,j)$ determined in the control region **A** (circles) and in the signal region (squares) from the MC study carried out at generator level with the exclusive MC sample of QCD multijet events resulting from $gg(q\bar{q}) \to b\bar{b}$ production mechanisms. The bin notation follows the definition presented in figure 2. The vertical bars include both statistical and systematic uncertainties.

7.1 Uncertainties related to background

The estimation of the QCD multijet background is based solely on data and is therefore not affected by imperfections in the simulation of the detector response and inaccuracies in the modelling of the muon and track reconstruction.

The shape of the background in the two-dimensional (m_1, m_2) distribution is modelled according to eq. (6.2). The uncertainty in the two-dimensional shape $f_{2D}(m_1, m_2)$ is dominated by uncertainties in the correlation coefficients $C(i,j)$ derived in the QCD multijet background-enriched control region **A** as described in section 6. The statistical uncertainties in $C(i,j)$ in region **A** range from 2 to 14%, as seen in figure 5. These uncertainties are accounted for in the signal extraction procedure by 10 independent nuisance parameters, one nuisance parameter per bin in the (m_1, m_2) distribution. The systematic uncertainties related to the extrapolation of $C(i,j)$ from the control region **A** to the signal region are derived from the dedicated MC study. The correlation coefficients are found to be compatible between the signal region and the control region **A** within uncertainties ranging from 2 to 22% (Figure 6). These uncertainties are accounted for by 10 additional independent nuisance parameters.

The possible contamination of control region **A** by the signal may bias the estimation of the correlation coefficients and consequently have an impact on the evaluation of the QCD multijet background. The effect is estimated with a conservative assumption on the branching fraction $\mathcal{B}(H(125) \to \phi_1\phi_1)\,\mathcal{B}^2(\phi_1 \to \tau\tau)$ of 32%, which corresponds to the 95% confidence level (CL) upper limit set by CMS on the branching fraction of the H(125) boson decays to non-standard model particles [4], while the cross section for gluon-gluon fusion

Source	Value	Affected sample	Type	Effect on the total yield
Statistical uncertainties in $C(i,j)$	2–14%	bkg.	bin-by-bin	—
Extrapolation uncertainties in $C(i,j)$	2–22%	bkg.	bin-by-bin	—
Integrated luminosity	2.6%	signal	norm.	2.6%
Muon ID and trigger efficiency	2% per muon	signal	norm.	4%
Track selection and isolation efficiency	5% per track	signal	norm.	10%
MC statistical uncertainties	7–100%	signal	bin-by-bin	4–6%
Theory uncertainties in the signal acceptance				
μ_r and μ_f variations	1%	signal	norm.	1%
PDF	1%	signal	norm.	1%
Effect of b quark loop contribution to gg $\rightarrow$ H(125)	3%	signal	norm.	3%

Table 2. Systematic uncertainties and their effect on the estimates of the QCD multijet background and signal. The effect of the uncertainties in $C(i,j)$ on the total background yield is absorbed by the overall background normalization, which is allowed to vary freely in the fit.

is set to the value predicted in the standard model (19.3 pb). Under these assumptions, the contamination of region **A** by the signal is estimated to be less than 2% for all mass hypotheses m_{ϕ_1} and in all bins of the two-dimensional (m_1, m_2) distribution, with the exception of bin (4,4), where the contamination can reach 12% for $m_{\phi_1} = 8\,\mathrm{GeV}$. However, the overall effect on the signal extraction is found to be marginal. Within this conservative scenario, variations of $C(i,j)$ due to possible contamination of control region **A** by the signal modify the observed and expected upper limits at 95% CL on $(\sigma\mathcal{B})_\mathrm{sig}$ by less than 1% for all considered values of m_{ϕ_1}.

7.2 Uncertainties related to signal

The following uncertainties in the signal estimate are taken into account, and are summarized in table 2.

An uncertainty of 2.6% is assigned to the integrated luminosity estimate [64].

The uncertainty in the muon identification and trigger efficiency is estimated to be 2% using the tag-and-probe technique applied to a sample of Z $\rightarrow \mu\mu$ decays. Because final states with two muons are selected in this analysis, this uncertainty translates into a 4% systematic uncertainty in the signal acceptance.

The track selection and isolation efficiency is assessed with a study performed on a sample of Z bosons decaying into a pair of τ leptons. In the selected $Z \to \tau\tau$ events, one τ lepton is identified via its muonic decay, while the other is identified as an isolated track resulting from a one-prong decay. The track is required to pass the nominal selection criteria used in the main analysis. From this study the uncertainty in the track selection and isolation efficiency is estimated to be 5%. As the analysis requires each muon to be accompanied by one track, this uncertainty gives rise to a 10% systematic uncertainty in the signal acceptance.

The muon momentum and track momentum scale uncertainties are smaller than 0.5% and have a negligible effect on the analysis.

The bin-by-bin MC statistical uncertainties in the signal acceptance range from 7 to 100%. Their impact on the signal normalization is between 4 and 6% as indicated in table 1. These uncertainties are accounted for in the signal extraction procedure by 10 nuisance parameters, corresponding to 10 independent bins in the (m_1, m_2) distribution.

Theoretical uncertainties have an impact on the differential kinematic distributions of the produced H(125) boson, in particular its p_T spectrum, thereby affecting signal acceptance. The uncertainty due to missing higher-order corrections to the gluon-gluon fusion process are estimated with the HqT program by varying the renormalization (μ_r) and factorization (μ_f) scales. The H(125) p_T-dependent k factors are recomputed according to these variations and applied to the simulated signal samples. The resulting effect on the signal acceptance is estimated to be of the order of 1%.

The HqT program is also used to evaluate the effect of the PDF uncertainties. The nominal k factors for the H(125) boson p_T spectrum are computed with the MSTW2008nnlo PDF set [65]. Variations of the MSTW2008nnlo PDFs within their uncertainties change the signal acceptance by about 1%, whilst using the CTEQ6L1 PDF set changes the signal acceptance by about 0.7%. These variations are covered by the assigned uncertainty of 1%.

The contribution of b quark loops to the gluon-gluon fusion process depends on the NMSSM parameters, in particular $\tan\beta$, the ratio of the vacuum expectation values of the two NMSSM Higgs doublets. The corresponding uncertainty is conservatively estimated by calculating k factors for the H(125) boson p_T spectrum with POWHEG [66–69], removing any contribution from the top quark loop and retaining only the contribution from the b quark loop. The modified k factors applied to the simulated signal samples change the signal acceptance by approximately 3% for all mass hypotheses m_{ϕ_1}.

8 Results

The signal is extracted with a binned maximum-likelihood fit applied to the two-dimensional (m_1, m_2) distribution in data. For each mass hypothesis of the ϕ_1 boson, the (m_1, m_2) distribution in data is fitted with the QCD multijet background shape and the gg $\to$ H(125) signal shape for the ϕ_1 mass under test. The contribution to the final selected sample from vector boson fusion and vector boson associated production of the H(125) boson is suppressed by the selection described in section 4, i.e. by the requirement $\Delta R(\mu, \mu) > 2$. The impact of other backgrounds on the fit is found to be negligible. The signal shapes are derived from simulation. The background shape is evaluated from data,
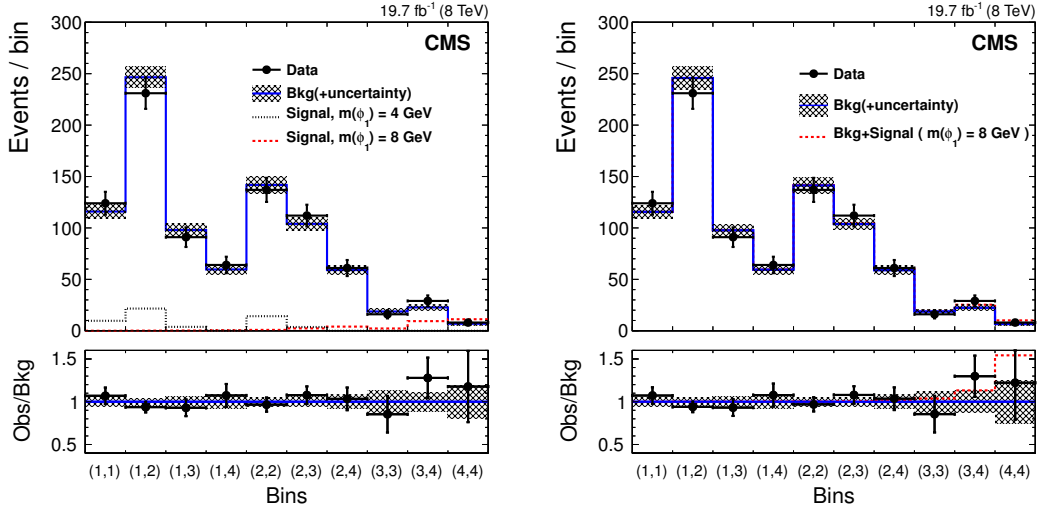
Figure 7. The two-dimensional (m_1, m_2) distribution unrolled into a one-dimensional array of analysis bins. In the left plot, data (points) are compared with the background prediction (solid histogram) after applying the maximum-likelihood fit under the background-only hypothesis and with the signal expectation for two mass hypotheses, $m_{\phi_1} = 4$ and $8\,\text{GeV}$ (dotted and dashed histograms, respectively). The signal distributions are obtained from simulation and normalized to a value of the cross section times branching fraction of $5\,\text{pb}$. In the right plot, data (points) are compared with the background prediction (solid histogram) and the background+signal prediction for $m_{\phi_1} = 8\,\text{GeV}$ (dashed histogram) after applying the maximum-likelihood fit under the signal+background hypothesis. The bin notation follows the definition presented in figure 2.

as described in section 6. The systematic uncertainties are accounted for in the fit via nuisance parameters with log-normal pdfs.

The contribution to the final selected sample from vector boson fusion (qqH) and vector boson associated production (VH) of the H(125) boson is suppressed by the selection described in section 4, especially by the requirement $\Delta R(\mu, \mu) > 2$. For the values of the H(125) boson production cross sections predicted in the SM, the expected contribution from the qqH and VH processes to the final selected sample is estimated to be less than 4% of total signal yield for all tested m_{ϕ_1} hypotheses. The shapes of the two-dimensional (m_1, m_2) distributions are found to be nearly indistinguishable among the three considered production modes, making it difficult to extract individual contributions from these processes in a model independent way. In the following these contributions are neglected, resulting in more conservative upper limits on $(\sigma\mathcal{B})_\text{sig}$. Subtraction of the qqH and VH contributions assuming the SM cross sections for the H(125) production mechanisms would decrease the upper limits on $(\sigma\mathcal{B})_\text{sig}$ by less than 4% for all tested values of m_{ϕ_1}.

First, the data are examined for their consistency with the background-only hypothesis by means of a fit performed with the normalization of the signal fixed to zero. Figure 7 (left) shows the two-dimensional (m_1, m_2) distribution unrolled into a one-dimensional array of analysis bins after performing the maximum-likelihood fit under the background-only hypothesis. The signal distribution, although not used in the fit, is also included for comparison, for the mass hypotheses $m_{\phi_1} = 4$ and $8\,\text{GeV}$.

Bin	Data	Bkg.	Signal for $(\sigma\mathcal{B})_{\text{sig}} = 5\,\text{pb}$, $m_{\phi_1} =$				
			4 GeV	5 GeV	6 GeV	7 GeV	8 GeV
(1,1)	124	116 ± 7	9.7 ± 1.5	1.9 ± 0.5	<0.1	0.1 ± 0.1	<0.1
(1,2)	231	247 ± 10	21.6 ± 2.9	6.8 ± 1.1	1.9 ± 0.5	0.3 ± 0.2	0.1 ± 0.1
(1,3)	91	98 ± 6	3.8 ± 0.8	4.9 ± 0.9	2.4 ± 0.6	0.9 ± 0.3	0.2 ± 0.2
(1,4)	64	60 ± 5	0.1 ± 0.1	1.5 ± 0.4	1.8 ± 0.5	0.8 ± 0.3	0.5 ± 0.2
(2,2)	137	142 ± 8	14.2 ± 2.0	8.2 ± 1.3	2.8 ± 0.6	1.5 ± 0.4	0.8 ± 0.3
(2,3)	112	104 ± 6	3.7 ± 0.7	10.4 ± 1.6	9.2 ± 1.4	4.4 ± 0.8	2.3 ± 0.6
(2,4)	61	59 ± 5	<0.1	2.6 ± 0.6	5.6 ± 1.0	8.1 ± 1.3	4.0 ± 0.8
(3,3)	16	19 ± 2	<0.1	4.8 ± 0.9	4.8 ± 0.9	3.7 ± 0.7	2.2 ± 0.5
(3,4)	29	23 ± 3	<0.1	1.9 ± 0.5	8.0 ± 0.9	11.1 ± 1.5	9.4 ± 1.4
(4,4)	8	7 ± 1	<0.1	<0.1	3.1 ± 0.6	9.1 ± 1.4	11.2 ± 1.7

Table 3. The number of observed data events, the predicted background yields, and the expected signal yields, for different masses of the ϕ_1 boson in individual bins of the (m_1, m_2) distribution. The background yields and uncertainties are obtained from the maximum-likelihood fit under the background-only hypothesis. The signal yields are obtained from simulation and normalized to a signal cross section times branching fraction of 5 pb. The uncertainties in the signal yields include systematic and MC statistical uncertainties. The bin notation follows the definition presented in figure 2.

Table 3 presents the number of observed data events, the predicted background yields obtained from a fit under the background-only hypothesis, and the expected signal yields obtained from simulation, for each unique bin in the two-dimensional (m_1, m_2) distribution. The data are well described by the background-only model.

The signal cross section times branching fraction is constrained by performing a fit under the signal+background hypothesis, where both the background and signal normalisations are allowed to vary freely in the fit. A representative example of the fit under the signal+background hypothesis at $m_{\phi_1} = 8\,\text{GeV}$ is presented in figure 7 (right). No significant deviations from the background expectation are observed in data. Only a small excess is found for $6 \leq m_{\phi_1} \leq 8\,\text{GeV}$, with a local significance ranging between 1.2σ ($m_{\phi_1} = 8\,\text{GeV}$) and 1.4σ ($m_{\phi_1} = 6\,\text{GeV}$). Results of the analysis are used to set upper limits on $(\sigma\mathcal{B})_{\text{sig}}$ at 95% CL. The modified frequentist CL_s criterion [70, 71], implemented in the ROOSTATS package [72], is used for the calculation of the exclusion limits. Figure 8 shows the observed upper limit on $(\sigma\mathcal{B})_{\text{sig}}$ at 95% CL, together with the expected limit obtained under the background-only hypothesis, for m_{ϕ_1} in the range from 4 to 8 GeV. Exclusion limits are also reported in table 4.

The observed limit is compatible with the expected limit within two standard deviations in the entire tested range of the ϕ_1 boson mass, $4 \leq m_{\phi_1} \leq 8\,\text{GeV}$. The observed limit ranges from 4.5 pb at $m_{\phi_1} = 8\,\text{GeV}$ to 10.3 pb at $m_{\phi_1} = 5\,\text{GeV}$. The expected limit ranges from 2.9 pb at $m_{\phi_1} = 8\,\text{GeV}$ to 10.6 pb at $m_{\phi_1} = 4\,\text{GeV}$.
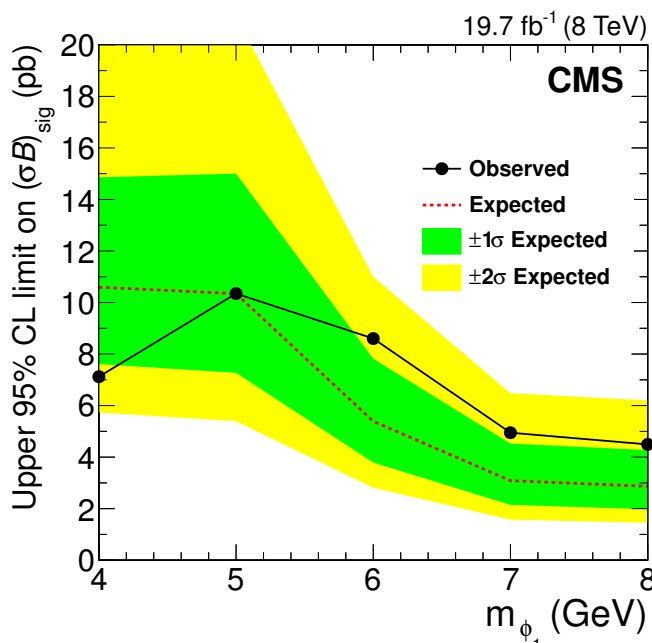
Figure 8. The observed and expected upper limits on $(\sigma\mathcal{B})_{\mathrm{sig}}$ in pb at 95% CL, as a function of m_{ϕ_1}. The expected limit is obtained under the background-only hypothesis. The bands show the expected $\pm 1\sigma$ and $\pm 2\sigma$ probability intervals around the expected limit.

m_{ϕ_1} [GeV]	Upper limits on $(\sigma\mathcal{B})_{\mathrm{sig}}$ [pb] at 95% CL					
	observed	-2σ	-1σ	expected	$+1\sigma$	$+2\sigma$
4	7.1	5.7	7.6	10.6	14.9	20.2
5	10.3	5.4	7.3	10.3	15.0	21.2
6	8.6	2.8	3.8	5.4	7.8	11.0
7	5.0	1.6	2.2	3.1	4.5	6.5
8	4.5	1.5	2.0	2.9	4.3	6.2

Table 4. The observed upper limit on $(\sigma\mathcal{B})_{\mathrm{sig}}$ at 95% CL, together with the expected limit obtained in the background-only hypothesis, as a function of m_{ϕ_1}. Also shown are $\pm 1\sigma$ and $\pm 2\sigma$ probability intervals around the expected limit.

The analysis presented here complements the search for $\mathrm{h/H} \to \mathrm{a_1 a_1} \to \mu\mu\tau\tau$ performed by the ATLAS Collaboration [52], providing results in the 4τ channel, which has not been previously explored at the LHC.

9   Summary

A search for a very light NMSSM Higgs boson $\mathrm{a_1}$ or $\mathrm{h_1}$, produced in decays of the observed boson with a mass near 125 GeV, H(125), is performed on a pp collision data set corresponding to an integrated luminosity of $19.7\,\mathrm{fb}^{-1}$, collected at a centre-of-mass energy of 8 TeV. The analysis searches for the production of an H(125) boson via gluon-gluon fusion,

and its decay into a pair of a_1 (h_1) states, each of which decays into a pair of τ leptons. The search covers a mass range of the a_1 (h_1) boson of 4 to 8 GeV. No significant excess above background expectations is found in data, and upper limits at 95% CL are set on the signal production cross section times branching fraction,

$$(\sigma\mathcal{B})_{\text{sig}} \equiv \sigma(\text{gg} \to \text{H}(125)) \, \mathcal{B}(\text{H}(125) \to \phi_1\phi_1) \, \mathcal{B}^2(\phi_1 \to \tau\tau),$$

where ϕ_1 is either the a_1 or h_1 boson. The observed upper limit at 95% CL on $(\sigma\mathcal{B})_{\text{sig}}$ ranges from 4.5 pb at $m_{\phi_1} = 8$ GeV to 10.3 pb at $m_{\phi_1} = 5$ GeV.

Acknowledgments

References

[1] ATLAS collaboration, *Observation of a new particle in the search for the Standard Model Higgs boson with the ATLAS detector at the LHC*, *Phys. Lett.* **B 716** (2012) 1 [arXiv:1207.7214] [INSPIRE].

[2] CMS collaboration, *Observation of a new boson at a mass of* 125 *GeV with the CMS experiment at the LHC*, *Phys. Lett.* **B 716** (2012) 30 [arXiv:1207.7235] [INSPIRE].

[3] CMS collaboration, *Observation of a new boson with mass near* 125 *GeV in pp collisions at* $\sqrt{s} = 7$ *and* 8 *TeV*, *JHEP* **06** (2013) 081 [arXiv:1303.4571] [INSPIRE].

[4] CMS collaboration, *Precise determination of the mass of the Higgs boson and tests of compatibility of its couplings with the standard model predictions using proton collisions at* 7 *and* 8 *TeV*, *Eur. Phys. J.* **C 75** (2015) 212 [arXiv:1412.8662] [INSPIRE].

[5] CMS collaboration, *Observation of the diphoton decay of the Higgs boson and measurement of its properties*, *Eur. Phys. J.* **C 74** (2014) 3076 [arXiv:1407.0558] [INSPIRE].

[6] CMS collaboration, *Measurement of the properties of a Higgs boson in the four-lepton final state*, *Phys. Rev.* **D 89** (2014) 092007 [arXiv:1312.5353] [INSPIRE].

[7] CMS collaboration, *Measurement of Higgs boson production and properties in the WW decay channel with leptonic final states*, *JHEP* **01** (2014) 096 [arXiv:1312.1129] [INSPIRE].

[8] CMS collaboration, *Evidence for the 125 GeV Higgs boson decaying to a pair of τ leptons*, *JHEP* **05** (2014) 104 [arXiv:1401.5041] [INSPIRE].

[9] CMS collaboration, *Evidence for the direct decay of the 125 GeV Higgs boson to fermions*, *Nature Phys.* **10** (2014) 557 [arXiv:1401.6527] [INSPIRE].

[10] ATLAS collaboration, *Measurement of Higgs boson production in the diphoton decay channel in pp collisions at center-of-mass energies of 7 and 8 TeV with the ATLAS detector*, *Phys. Rev.* **D 90** (2014) 112015 [arXiv:1408.7084] [INSPIRE].

[11] ATLAS collaboration, *Measurements of Higgs boson production and couplings in the four-lepton channel in pp collisions at center-of-mass energies of 7 and 8 TeV with the ATLAS detector*, *Phys. Rev.* **D 91** (2015) 012006 [arXiv:1408.5191] [INSPIRE].

[12] ATLAS collaboration, *Observation and measurement of Higgs boson decays to WW* with the ATLAS detector*, *Phys. Rev.* **D 92** (2015) 012006 [arXiv:1412.2641] [INSPIRE].

[13] ATLAS collaboration, *Evidence for the Higgs-boson Yukawa coupling to τ leptons with the ATLAS detector*, *JHEP* **04** (2015) 117 [arXiv:1501.04943] [INSPIRE].

[14] ATLAS collaboration, *Measurement of the Higgs boson mass from the $H \to \gamma\gamma$ and $H \to ZZ^* \to 4\ell$ channels with the ATLAS detector using $25\,fb^{-1}$ of pp collision data*, *Phys. Rev.* **D 90** (2014) 052004 [arXiv:1406.3827] [INSPIRE].

[15] Yu. A. Golfand and E.P. Likhtman, *Extension of the algebra of Poincaré group generators and violation of P invariance*, *JETP Lett.* **13** (1971) 323 [INSPIRE].

[16] J. Wess and B. Zumino, *Supergauge transformations in four-dimensions*, *Nucl. Phys.* **B 70** (1974) 39 [INSPIRE].

[17] J.R. Ellis, *Limits of the standard model*, hep-ph/0211168 [INSPIRE].

[18] P. Fayet, *Supergauge invariant extension of the Higgs mechanism and a model for the electron and its neutrino*, *Nucl. Phys.* **B 90** (1975) 104 [INSPIRE].

[19] P. Fayet, *Spontaneously broken supersymmetric theories of weak, electromagnetic and strong interactions*, *Phys. Lett.* **B 69** (1977) 489 [INSPIRE].

[20] R.K. Kaul and P. Majumdar, *Cancellation of quadratically divergent mass corrections in globally supersymmetric spontaneously broken gauge theories*, *Nucl. Phys.* **B 199** (1982) 36 [INSPIRE].

[21] R. Barbieri, S. Ferrara and C.A. Savoy, *Gauge models with spontaneously broken local supersymmetry*, *Phys. Lett.* **B 119** (1982) 343 [INSPIRE].

[22] H.P. Nilles, M. Srednicki and D. Wyler, *Weak interaction breakdown induced by supergravity*, *Phys. Lett.* **B 120** (1983) 346 [INSPIRE].

[23] J.M. Frere, D.R.T. Jones and S. Raby, *Fermion masses and induction of the weak scale by supergravity*, *Nucl. Phys.* **B 222** (1983) 11 [INSPIRE].

[24] J.P. Derendinger and C.A. Savoy, *Quantum effects and* SU(2) × U(1) *breaking in supergravity gauge theories*, *Nucl. Phys.* **B 237** (1984) 307 [ɪɴSPIRE].

[25] U. Ellwanger, C. Hugonie and A.M. Teixeira, *The next-to-minimal supersymmetric standard model*, *Phys. Rept.* **496** (2010) 1 [arXiv:0910.1785] [ɪɴSPIRE].

[26] M. Maniatis, *The next-to-minimal supersymmetric extension of the standard model reviewed*, *Int. J. Mod. Phys.* **A 25** (2010) 3505 [arXiv:0906.0777] [ɪɴSPIRE].

[27] J.E. Kim and H.P. Nilles, *The μ problem and the strong CP problem*, *Phys. Lett.* **B 138** (1984) 150 [ɪɴSPIRE].

[28] J.A. Casas, J.R. Espinosa and I. Hidalgo, *The MSSM fine tuning problem: a way out*, *JHEP* **01** (2004) 008 [hep-ph/0310137] [ɪɴSPIRE].

[29] R. Dermisek and J.F. Gunion, *Escaping the large fine tuning and little hierarchy problems in the next to minimal supersymmetric model and* h → aa *decays*, *Phys. Rev. Lett.* **95** (2005) 041801 [hep-ph/0502105] [ɪɴSPIRE].

[30] R. Dermisek and J.F. Gunion, *The NMSSM solution to the fine-tuning problem, precision electroweak constraints and the largest LEP Higgs event excess*, *Phys. Rev.* **D 76** (2007) 095006 [arXiv:0705.4387] [ɪɴSPIRE].

[31] G. Bélanger, U. Ellwanger, J.F. Gunion, Y. Jiang, S. Kraml and J.H. Schwarz, *Higgs bosons at 98 and 125 GeV at LEP and the LHC*, *JHEP* **01** (2013) 069 [arXiv:1210.1976] [ɪɴSPIRE].

[32] G. Bélanger, U. Ellwanger, J.F. Gunion, Y. Jiang and S. Kraml, *Two Higgs bosons at the Tevatron and the LHC?*, arXiv:1208.4952 [ɪɴSPIRE].

[33] J.F. Gunion, Y. Jiang and S. Kraml, *Diagnosing degenerate Higgs bosons at 125 GeV*, *Phys. Rev. Lett.* **110** (2013) 051801 [arXiv:1208.1817] [ɪɴSPIRE].

[34] J.F. Gunion, Y. Jiang and S. Kraml, *Could two NMSSM Higgs bosons be present near 125 GeV?*, *Phys. Rev.* **D 86** (2012) 071702 [arXiv:1207.1545] [ɪɴSPIRE].

[35] S.F. King, M. Mühlleitner and R. Nevzorov, *NMSSM Higgs benchmarks near 125 GeV*, *Nucl. Phys.* **B 860** (2012) 207 [arXiv:1201.2671] [ɪɴSPIRE].

[36] S.F. King, M. Mühlleitner, R. Nevzorov and K. Walz, *Natural NMSSM Higgs bosons*, *Nucl. Phys.* **B 870** (2013) 323 [arXiv:1211.5074] [ɪɴSPIRE].

[37] D. Curtin et al., *Exotic decays of the 125 GeV Higgs boson*, *Phys. Rev.* **D 90** (2014) 075004 [arXiv:1312.4992] [ɪɴSPIRE].

[38] U. Ellwanger, J.F. Gunion and C. Hugonie, *Difficult scenarios for NMSSM Higgs discovery at the LHC*, *JHEP* **07** (2005) 041 [hep-ph/0503203] [ɪɴSPIRE].

[39] U. Ellwanger, J.F. Gunion, C. Hugonie and S. Moretti, *Towards a no lose theorem for NMSSM Higgs discovery at the LHC*, hep-ph/0305109 [ɪɴSPIRE].

[40] U. Ellwanger, J.F. Gunion, C. Hugonie and S. Moretti, *NMSSM Higgs discovery at the LHC*, in *Physics at TeV colliders, Les Houches workshop*, May 26–June 6, Les Houches, France (2003), hep-ph/0401228 [ɪɴSPIRE].

[41] A. Belyaev, S. Hesselbach, S. Lehti, S. Moretti, A. Nikitenko and C.H. Shepherd-Themistocleous, *The scope of the 4τ channel in Higgs-strahlung and vector boson fusion for the NMSSM no-lose theorem at the LHC*, arXiv:0805.3505 [ɪɴSPIRE].

[42] A. Belyaev, J. Pivarski, A. Safonov, S. Senkin and A. Tatarinov, *LHC discovery potential of the lightest NMSSM Higgs in the* h₁ → a₁a₁ → 4 *muons channel*, *Phys. Rev.* **D 81** (2010) 075021 [arXiv:1002.1956] [ɪɴSPIRE].

[43] M. Lisanti and J.G. Wacker, *Discovering the Higgs with low mass muon pairs*, *Phys. Rev.* **D 79** (2009) 115006 [arXiv:0903.1377] [INSPIRE].

[44] M.M. Almarashi and S. Moretti, *Scope of Higgs production in association with a bottom quark pair in probing the Higgs sector of the NMSSM at the LHC*, arXiv:1205.1683 [INSPIRE].

[45] M.M. Almarashi and S. Moretti, *LHC signals of a heavy CP-even higgs boson in the NMSSM via decays into a Z and a light CP-odd Higgs state*, *Phys. Rev.* **D 85** (2012) 017701 [arXiv:1109.1735] [INSPIRE].

[46] N.-E. Bomark, S. Moretti, S. Munir and L. Roszkowski, *Revisiting a light NMSSM pseudoscalar at the LHC*, PoS(Charged2014)029 [arXiv:1412.5815] [INSPIRE].

[47] S.F. King, M. Mühlleitner, R. Nevzorov and K. Walz, *Discovery prospects for NMSSM Higgs bosons at the high-energy Large Hadron Collider*, *Phys. Rev.* **D 90** (2014) 095014 [arXiv:1408.1120] [INSPIRE].

[48] OPAL collaboration, G. Abbiendi et al., *Search for a low mass CP odd Higgs boson in e^+e^- collisions with the OPAL detector at LEP-2*, *Eur. Phys. J.* **C 27** (2003) 483 [hep-ex/0209068] [INSPIRE].

[49] ALEPH collaboration, S. Schael et al., *Search for neutral Higgs bosons decaying into four taus at LEP2*, *JHEP* **05** (2010) 049 [arXiv:1003.0705] [INSPIRE].

[50] D0 collaboration, V.M. Abazov et al., *Search for NMSSM Higgs bosons in the $h \to aa \to \mu\mu\mu\mu$, $\mu\mu\tau\tau$ channels using $p\bar{p}$ collisions at $\sqrt{s} = 1.96$ TeV*, *Phys. Rev. Lett.* **103** (2009) 061801 [arXiv:0905.3381] [INSPIRE].

[51] CMS collaboration, *A search for pair production of new light bosons decaying into muons*, *Phys. Lett.* **B 752** (2016) 146 [arXiv:1506.00424] [INSPIRE].

[52] ATLAS collaboration, *Search for Higgs bosons decaying to aa in the $\mu\mu\tau\tau$ final state in pp collisions at $\sqrt{s} = 8$ TeV with the ATLAS experiment*, *Phys. Rev.* **D 92** (2015) 052002 [arXiv:1505.01609] [INSPIRE].

[53] CMS collaboration, *The CMS experiment at the CERN LHC*, 2008 *JINST* **3** S08004 [INSPIRE].

[54] T. Sjöstrand, S. Mrenna and P.Z. Skands, *PYTHIA 6.4 physics and manual*, *JHEP* **05** (2006) 026 [hep-ph/0603175] [INSPIRE].

[55] G. Bozzi, S. Catani, D. de Florian and M. Grazzini, *Transverse-momentum resummation and the spectrum of the Higgs boson at the LHC*, *Nucl. Phys.* **B 737** (2006) 73 [hep-ph/0508068] [INSPIRE].

[56] D. de Florian, G. Ferrera, M. Grazzini and D. Tommasini, *Transverse-momentum resummation: Higgs boson production at the Tevatron and the LHC*, *JHEP* **11** (2011) 064 [arXiv:1109.2109] [INSPIRE].

[57] J. Alwall, M. Herquet, F. Maltoni, O. Mattelaer and T. Stelzer, *MadGraph 5: going beyond*, *JHEP* **06** (2011) 128 [arXiv:1106.0522] [INSPIRE].

[58] R. Field, *Early LHC underlying event data — Findings and surprises*, in 22$^{\mathrm{nd}}$ *Hadron Collider Physics Symposium (HCP2010)*, W. Trischuk ed., Toronto, Canada (2010), arXiv:1010.3558 [INSPIRE].

[59] J. Pumplin, D.R. Stump, J. Huston, H.L. Lai, P.M. Nadolsky and W.K. Tung, *New generation of parton distributions with uncertainties from global QCD analysis*, *JHEP* **07** (2002) 012 [hep-ph/0201195] [INSPIRE].

[60] S. Jadach, Z. Was, R. Decker and J.H. Kuhn, *The τ decay library TAUOLA: version 2.4*, *Comput. Phys. Commun.* **76** (1993) 361 [INSPIRE].

[61] GEANT4 collaboration, S. Agostinelli et al., *GEANT4 — A simulation toolkit*, *Nucl. Instrum. Meth.* **A 506** (2003) 250 [INSPIRE].

[62] CMS collaboration, *Performance of CMS muon reconstruction in pp collision events at* $\sqrt{s} = 7$ *TeV*, 2012 *JINST* **7** P10002 [arXiv:1206.4071] [INSPIRE].

[63] CMS collaboration, *Description and performance of track and primary-vertex reconstruction with the CMS tracker*, 2014 *JINST* **9** P10009 [arXiv:1405.6569] [INSPIRE].

[64] CMS collaboration, *CMS luminosity based on pixel cluster counting — Summer 2013 update*, CMS-PAS-LUM-13-001 (2013).

[65] A.D. Martin, W.J. Stirling, R.S. Thorne and G. Watt, *Parton distributions for the LHC*, *Eur. Phys. J.* **C 63** (2009) 189 [arXiv:0901.0002] [INSPIRE].

[66] S. Alioli, P. Nason, C. Oleari and E. Re, *NLO Higgs boson production via gluon fusion matched with shower in POWHEG*, *JHEP* **04** (2009) 002 [arXiv:0812.0578] [INSPIRE].

[67] P. Nason, *A new method for combining NLO QCD with shower Monte Carlo algorithms*, *JHEP* **11** (2004) 040 [hep-ph/0409146] [INSPIRE].

[68] S. Frixione, P. Nason and C. Oleari, *Matching NLO QCD computations with Parton Shower simulations: the POWHEG method*, *JHEP* **11** (2007) 070 [arXiv:0709.2092] [INSPIRE].

[69] S. Alioli, P. Nason, C. Oleari and E. Re, *A general framework for implementing NLO calculations in shower Monte Carlo programs: the POWHEG BOX*, *JHEP* **06** (2010) 043 [arXiv:1002.2581] [INSPIRE].

[70] A.L. Read, *Presentation of search results: the CL(s) technique*, *J. Phys.* **G 28** (2002) 2693 [INSPIRE].

[71] T. Junk, *Confidence level computation for combining searches with small statistics*, *Nucl. Instrum. Meth.* **A 434** (1999) 435 [hep-ex/9902006] [INSPIRE].

[72] L. Moneta et al., *The RooStats Project*, PoS(ACAT2010)057 [arXiv:1009.1003] [INSPIRE].

The CMS collaboration

Yerevan Physics Institute, Yerevan, Armenia

V. Khachatryan, A.M. Sirunyan, A. Tumasyan

Institut für Hochenergiephysik der OeAW, Wien, Austria

W. Adam, E. Asilar, T. Bergauer, J. Brandstetter, E. Brondolin, M. Dragicevic, J. Erö, M. Flechl, M. Friedl, R. Frühwirth[1], V.M. Ghete, C. Hartl, N. Hörmann, J. Hrubec, M. Jeitler[1], V. Knünz, A. König, M. Krammer[1], I. Krätschmer, D. Liko, T. Matsushita, I. Mikulec, D. Rabady[2], B. Rahbaran, H. Rohringer, J. Schieck[1], R. Schöfbeck, J. Strauss, W. Treberer-Treberspurg, W. Waltenberger, C.-E. Wulz[1]

National Centre for Particle and High Energy Physics, Minsk, Belarus

V. Mossolov, N. Shumeiko, J. Suarez Gonzalez

Universiteit Antwerpen, Antwerpen, Belgium

S. Alderweireldt, T. Cornelis, E.A. De Wolf, X. Janssen, A. Knutsson, J. Lauwers, S. Luyckx, R. Rougny, M. Van De Klundert, H. Van Haevermaet, P. Van Mechelen, N. Van Remortel, A. Van Spilbeeck

Vrije Universiteit Brussel, Brussel, Belgium

S. Abu Zeid, F. Blekman, J. D'Hondt, N. Daci, I. De Bruyn, K. Deroover, N. Heracleous, J. Keaveney, S. Lowette, L. Moreels, A. Olbrechts, Q. Python, D. Strom, S. Tavernier, W. Van Doninck, P. Van Mulders, G.P. Van Onsem, I. Van Parijs

Université Libre de Bruxelles, Bruxelles, Belgium

P. Barria, H. Brun, C. Caillol, B. Clerbaux, G. De Lentdecker, G. Fasanella, L. Favart, A. Grebenyuk, G. Karapostoli, T. Lenzi, A. Léonard, T. Maerschalk, A. Marinov, L. Perniè, A. Randle-conde, T. Reis, T. Seva, C. Vander Velde, P. Vanlaer, R. Yonamine, F. Zenoni, F. Zhang[3]

Ghent University, Ghent, Belgium

K. Beernaert, L. Benucci, A. Cimmino, S. Crucy, D. Dobur, A. Fagot, G. Garcia, M. Gul, J. Mccartin, A.A. Ocampo Rios, D. Poyraz, D. Ryckbosch, S. Salva, M. Sigamani, N. Strobbe, M. Tytgat, W. Van Driessche, E. Yazgan, N. Zaganidis

Université Catholique de Louvain, Louvain-la-Neuve, Belgium

S. Basegmez, C. Beluffi[4], O. Bondu, S. Brochet, G. Bruno, A. Caudron, L. Ceard, G.G. Da Silveira, C. Delaere, D. Favart, L. Forthomme, A. Giammanco[5], J. Hollar, A. Jafari, P. Jez, M. Komm, V. Lemaitre, A. Mertens, C. Nuttens, L. Perrini, A. Pin, K. Piotrzkowski, A. Popov[6], L. Quertenmont, M. Selvaggi, M. Vidal Marono

Université de Mons, Mons, Belgium

N. Beliy, G.H. Hammad

Centro Brasileiro de Pesquisas Fisicas, Rio de Janeiro, Brazil

W.L. Aldá Júnior, G.A. Alves, L. Brito, M. Correa Martins Junior, M. Hamer, C. Hensel, C. Mora Herrera, A. Moraes, M.E. Pol, P. Rebello Teles

Universidade do Estado do Rio de Janeiro, Rio de Janeiro, Brazil

E. Belchior Batista Das Chagas, W. Carvalho, J. Chinellato[7], A. Custódio, E.M. Da Costa, D. De Jesus Damiao, C. De Oliveira Martins, S. Fonseca De Souza, L.M. Huertas Guativa, H. Malbouisson, D. Matos Figueiredo, L. Mundim, H. Nogima, W.L. Prado Da Silva, A. Santoro, A. Sznajder, E.J. Tonelli Manganote[7], A. Vilela Pereira

Universidade Estadual Paulista [a], Universidade Federal do ABC [b], São Paulo, Brazil

S. Ahuja[a], C.A. Bernardes[b], A. De Souza Santos[b], S. Dogra[a], T.R. Fernandez Perez Tomei[a], E.M. Gregores[b], P.G. Mercadante[b], C.S. Moon[a,8], S.F. Novaes[a], Sandra S. Padula[a], D. Romero Abad, J.C. Ruiz Vargas

Institute for Nuclear Research and Nuclear Energy, Sofia, Bulgaria

A. Aleksandrov, R. Hadjiiska, P. Iaydjiev, M. Rodozov, S. Stoykova, G. Sultanov, M. Vutova

University of Sofia, Sofia, Bulgaria

A. Dimitrov, I. Glushkov, L. Litov, B. Pavlov, P. Petkov

Institute of High Energy Physics, Beijing, China

M. Ahmad, J.G. Bian, G.M. Chen, H.S. Chen, M. Chen, T. Cheng, R. Du, C.H. Jiang, R. Plestina[9], F. Romeo, S.M. Shaheen, J. Tao, C. Wang, Z. Wang, H. Zhang

State Key Laboratory of Nuclear Physics and Technology, Peking University, Beijing, China

C. Asawatangtrakuldee, Y. Ban, Q. Li, S. Liu, Y. Mao, S.J. Qian, D. Wang, Z. Xu

Universidad de Los Andes, Bogota, Colombia

C. Avila, A. Cabrera, L.F. Chaparro Sierra, C. Florez, J.P. Gomez, B. Gomez Moreno, J.C. Sanabria

University of Split, Faculty of Electrical Engineering, Mechanical Engineering and Naval Architecture, Split, Croatia

N. Godinovic, D. Lelas, I. Puljak, P.M. Ribeiro Cipriano

University of Split, Faculty of Science, Split, Croatia

Z. Antunovic, M. Kovac

Institute Rudjer Boskovic, Zagreb, Croatia

V. Brigljevic, K. Kadija, J. Luetic, S. Micanovic, L. Sudic

University of Cyprus, Nicosia, Cyprus

A. Attikis, G. Mavromanolakis, J. Mousa, C. Nicolaou, F. Ptochos, P.A. Razis, H. Rykaczewski

Charles University, Prague, Czech Republic

M. Bodlak, M. Finger[10], M. Finger Jr.[10]

Academy of Scientific Research and Technology of the Arab Republic of Egypt, Egyptian Network of High Energy Physics, Cairo, Egypt

A.A. Abdelalim[11,12], A. Awad, A. Mahrous[11], A. Radi[13,14]

National Institute of Chemical Physics and Biophysics, Tallinn, Estonia

B. Calpas, M. Kadastik, M. Murumaa, M. Raidal, A. Tiko, C. Veelken

Department of Physics, University of Helsinki, Helsinki, Finland

P. Eerola, J. Pekkanen, M. Voutilainen

Helsinki Institute of Physics, Helsinki, Finland

J. Härkönen, V. Karimäki, R. Kinnunen, T. Lampén, K. Lassila-Perini, S. Lehti, T. Lindén, P. Luukka, T. Mäenpää, T. Peltola, E. Tuominen, J. Tuominiemi, E. Tuovinen, L. Wendland

Lappeenranta University of Technology, Lappeenranta, Finland

J. Talvitie, T. Tuuva

DSM/IRFU, CEA/Saclay, Gif-sur-Yvette, France

M. Besancon, F. Couderc, M. Dejardin, D. Denegri, B. Fabbro, J.L. Faure, C. Favaro, F. Ferri, S. Ganjour, A. Givernaud, P. Gras, G. Hamel de Monchenault, P. Jarry, E. Locci, M. Machet, J. Malcles, J. Rander, A. Rosowsky, M. Titov, A. Zghiche

Laboratoire Leprince-Ringuet, Ecole Polytechnique, IN2P3-CNRS, Palaiseau, France

I. Antropov, S. Baffioni, F. Beaudette, P. Busson, L. Cadamuro, E. Chapon, C. Charlot, T. Dahms, O. Davignon, N. Filipovic, A. Florent, R. Granier de Cassagnac, S. Lisniak, L. Mastrolorenzo, P. Miné, I.N. Naranjo, M. Nguyen, C. Ochando, G. Ortona, P. Paganini, P. Pigard, S. Regnard, R. Salerno, J.B. Sauvan, Y. Sirois, T. Strebler, Y. Yilmaz, A. Zabi

Institut Pluridisciplinaire Hubert Curien, Université de Strasbourg, Université de Haute Alsace Mulhouse, CNRS/IN2P3, Strasbourg, France

J.-L. Agram[15], J. Andrea, A. Aubin, D. Bloch, J.-M. Brom, M. Buttignol, E.C. Chabert, N. Chanon, C. Collard, E. Conte[15], X. Coubez, J.-C. Fontaine[15], D. Gelé, U. Goerlach, C. Goetzmann, A.-C. Le Bihan, J.A. Merlin[2], K. Skovpen, P. Van Hove

Centre de Calcul de l'Institut National de Physique Nucleaire et de Physique des Particules, CNRS/IN2P3, Villeurbanne, France

S. Gadrat

Université de Lyon, Université Claude Bernard Lyon 1, CNRS-IN2P3, Institut de Physique Nucléaire de Lyon, Villeurbanne, France

S. Beauceron, C. Bernet, G. Boudoul, E. Bouvier, C.A. Carrillo Montoya, R. Chierici, D. Contardo, B. Courbon, P. Depasse, H. El Mamouni, J. Fan, J. Fay, S. Gascon, M. Gouzevitch, B. Ille, F. Lagarde, I.B. Laktineh, M. Lethuillier, L. Mirabito, A.L. Pequegnot, S. Perries, J.D. Ruiz Alvarez, D. Sabes, L. Sgandurra, V. Sordini, M. Vander Donckt, P. Verdier, S. Viret

Georgian Technical University, Tbilisi, Georgia

T. Toriashvili[16]

Tbilisi State University, Tbilisi, Georgia

Z. Tsamalaidze[10]

RWTH Aachen University, I. Physikalisches Institut, Aachen, Germany

C. Autermann, S. Beranek, M. Edelhoff, L. Feld, A. Heister, M.K. Kiesel, K. Klein, M. Lipinski, A. Ostapchuk, M. Preuten, F. Raupach, S. Schael, J.F. Schulte, T. Verlage, H. Weber, B. Wittmer, V. Zhukov[6]

RWTH Aachen University, III. Physikalisches Institut A, Aachen, Germany

M. Ata, M. Brodski, E. Dietz-Laursonn, D. Duchardt, M. Endres, M. Erdmann, S. Erdweg, T. Esch, R. Fischer, A. Güth, T. Hebbeker, C. Heidemann, K. Hoepfner, D. Klingebiel, S. Knutzen, P. Kreuzer, M. Merschmeyer, A. Meyer, P. Millet, M. Olschewski, K. Padeken, P. Papacz, T. Pook, M. Radziej, H. Reithler, M. Rieger, F. Scheuch, L. Sonnenschein, D. Teyssier, S. Thüer

RWTH Aachen University, III. Physikalisches Institut B, Aachen, Germany

V. Cherepanov, Y. Erdogan, G. Flügge, H. Geenen, M. Geisler, F. Hoehle, B. Kargoll, T. Kress, Y. Kuessel, A. Künsken, J. Lingemann[2], A. Nehrkorn, A. Nowack, I.M. Nugent, C. Pistone, O. Pooth, A. Stahl

Deutsches Elektronen-Synchrotron, Hamburg, Germany

M. Aldaya Martin, I. Asin, N. Bartosik, O. Behnke, U. Behrens, A.J. Bell, A. Bethani, K. Borras[17], A. Burgmeier, A. Cakir, L. Calligaris, A. Campbell, S. Choudhury[18], F. Costanza, C. Diez Pardos, G. Dolinska, S. Dooling, T. Dorland, G. Eckerlin, D. Eckstein, T. Eichhorn, G. Flucke, E. Gallo[19], J. Garay Garcia, A. Geiser, A. Gizhko, P. Gunnellini, J. Hauk, M. Hempel[20], H. Jung, A. Kalogeropoulos, O. Karacheban[20], M. Kasemann, P. Katsas, J. Kieseler, C. Kleinwort, I. Korol, W. Lange, J. Leonard, K. Lipka, A. Lobanov, W. Lohmann[20], R. Mankel, I. Marfin[20], I.-A. Melzer-Pellmann, A.B. Meyer, G. Mittag, J. Mnich, A. Mussgiller, S. Naumann-Emme, A. Nayak, E. Ntomari, H. Perrey, D. Pitzl, R. Placakyte, A. Raspereza, B. Roland, M.Ö. Sahin, P. Saxena, T. Schoerner-Sadenius, M. Schröder, C. Seitz, S. Spannagel, K.D. Trippkewitz, R. Walsh, C. Wissing

University of Hamburg, Hamburg, Germany

V. Blobel, M. Centis Vignali, A.R. Draeger, J. Erfle, E. Garutti, K. Goebel, D. Gonzalez, M. Görner, J. Haller, M. Hoffmann, R.S. Höing, A. Junkes, R. Klanner, R. Kogler, T. Lapsien, T. Lenz, I. Marchesini, D. Marconi, M. Meyer, D. Nowatschin, J. Ott, F. Pantaleo[2], T. Peiffer, A. Perieanu, N. Pietsch, J. Poehlsen, D. Rathjens, C. Sander, H. Schettler, P. Schleper, E. Schlieckau, A. Schmidt, J. Schwandt, M. Seidel, V. Sola, H. Stadie, G. Steinbrück, H. Tholen, D. Troendle, E. Usai, L. Vanelderen, A. Vanhoefer, B. Vormwald

Institut für Experimentelle Kernphysik, Karlsruhe, Germany

M. Akbiyik, C. Barth, C. Baus, J. Berger, C. Böser, E. Butz, T. Chwalek, F. Colombo, W. De Boer, A. Descroix, A. Dierlamm, S. Fink, F. Frensch, M. Giffels, A. Gilbert,

F. Hartmann[2], S.M. Heindl, U. Husemann, I. Katkov[6], A. Kornmayer[2], P. Lobelle Pardo, B. Maier, H. Mildner, M.U. Mozer, T. Müller, Th. Müller, M. Plagge, G. Quast, K. Rabbertz, S. Röcker, F. Roscher, H.J. Simonis, F.M. Stober, R. Ulrich, J. Wagner-Kuhr, S. Wayand, M. Weber, T. Weiler, C. Wöhrmann, R. Wolf

Institute of Nuclear and Particle Physics (INPP), NCSR Demokritos, Aghia Paraskevi, Greece

G. Anagnostou, G. Daskalakis, T. Geralis, V.A. Giakoumopoulou, A. Kyriakis, D. Loukas, A. Psallidas, I. Topsis-Giotis

University of Athens, Athens, Greece

A. Agapitos, S. Kesisoglou, A. Panagiotou, N. Saoulidou, E. Tziaferi

University of Ioánnina, Ioánnina, Greece

I. Evangelou, G. Flouris, C. Foudas, P. Kokkas, N. Loukas, N. Manthos, I. Papadopoulos, E. Paradas, J. Strologas

Wigner Research Centre for Physics, Budapest, Hungary

G. Bencze, C. Hajdu, A. Hazi, P. Hidas, D. Horvath[21], F. Sikler, V. Veszpremi, G. Vesztergombi[22], A.J. Zsigmond

Institute of Nuclear Research ATOMKI, Debrecen, Hungary

N. Beni, S. Czellar, J. Karancsi[23], J. Molnar, Z. Szillasi

University of Debrecen, Debrecen, Hungary

M. Bartók[24], A. Makovec, P. Raics, Z.L. Trocsanyi, B. Ujvari

National Institute of Science Education and Research, Bhubaneswar, India

P. Mal, K. Mandal, D.K. Sahoo, N. Sahoo, S.K. Swain

Panjab University, Chandigarh, India

S. Bansal, S.B. Beri, V. Bhatnagar, R. Chawla, R. Gupta, U.Bhawandeep, A.K. Kalsi, A. Kaur, M. Kaur, R. Kumar, A. Mehta, M. Mittal, J.B. Singh, G. Walia

University of Delhi, Delhi, India

Ashok Kumar, A. Bhardwaj, B.C. Choudhary, R.B. Garg, A. Kumar, S. Malhotra, M. Naimuddin, N. Nishu, K. Ranjan, R. Sharma, V. Sharma

Saha Institute of Nuclear Physics, Kolkata, India

S. Bhattacharya, K. Chatterjee, S. Dey, S. Dutta, Sa. Jain, N. Majumdar, A. Modak, K. Mondal, S. Mukherjee, S. Mukhopadhyay, A. Roy, D. Roy, S. Roy Chowdhury, S. Sarkar, M. Sharan

Bhabha Atomic Research Centre, Mumbai, India

A. Abdulsalam, R. Chudasama, D. Dutta, V. Jha, V. Kumar, A.K. Mohanty[2], L.M. Pant, P. Shukla, A. Topkar

Tata Institute of Fundamental Research, Mumbai, India

T. Aziz, S. Banerjee, S. Bhowmik[25], R.M. Chatterjee, R.K. Dewanjee, S. Dugad, S. Ganguly, S. Ghosh, M. Guchait, A. Gurtu[26], G. Kole, S. Kumar, B. Mahakud, M. Maity[25],

G. Majumder, K. Mazumdar, S. Mitra, G.B. Mohanty, B. Parida, T. Sarkar[25], N. Sur, B. Sutar, N. Wickramage[27]

Indian Institute of Science Education and Research (IISER), Pune, India
S. Chauhan, S. Dube, S. Sharma

Institute for Research in Fundamental Sciences (IPM), Tehran, Iran
H. Bakhshiansohi, H. Behnamian, S.M. Etesami[28], A. Fahim[29], R. Goldouzian, M. Khakzad, M. Mohammadi Najafabadi, M. Naseri, S. Paktinat Mehdiabadi, F. Rezaei Hosseinabadi, B. Safarzadeh[30], M. Zeinali

University College Dublin, Dublin, Ireland
M. Felcini, M. Grunewald

INFN Sezione di Bari [a], Università di Bari [b], Politecnico di Bari [c], Bari, Italy
M. Abbrescia[a,b], C. Calabria[a,b], C. Caputo[a,b], A. Colaleo[a], D. Creanza[a,c], L. Cristella[a,b], N. De Filippis[a,c], M. De Palma[a,b], L. Fiore[a], G. Iaselli[a,c], G. Maggi[a,c], M. Maggi[a], G. Miniello[a,b], S. My[a,c], S. Nuzzo[a,b], A. Pompili[a,b], G. Pugliese[a,c], R. Radogna[a,b], A. Ranieri[a], G. Selvaggi[a,b], L. Silvestris[a,2], R. Venditti[a,b], P. Verwilligen[a]

INFN Sezione di Bologna [a], Università di Bologna [b], Bologna, Italy
G. Abbiendi[a], C. Battilana[2], A.C. Benvenuti[a], D. Bonacorsi[a,b], S. Braibant-Giacomelli[a,b], L. Brigliadori[a,b], R. Campanini[a,b], P. Capiluppi[a,b], A. Castro[a,b], F.R. Cavallo[a], S.S. Chhibra[a,b], G. Codispoti[a,b], M. Cuffiani[a,b], G.M. Dallavalle[a], F. Fabbri[a], A. Fanfani[a,b], D. Fasanella[a,b], P. Giacomelli[a], C. Grandi[a], L. Guiducci[a,b], S. Marcellini[a], G. Masetti[a], A. Montanari[a], F.L. Navarria[a,b], A. Perrotta[a], A.M. Rossi[a,b], T. Rovelli[a,b], G.P. Siroli[a,b], N. Tosi[a,b], R. Travaglini[a,b]

INFN Sezione di Catania [a], Università di Catania [b], Catania, Italy
G. Cappello[a], M. Chiorboli[a,b], S. Costa[a,b], F. Giordano[a,b], R. Potenza[a,b], A. Tricomi[a,b], C. Tuve[a,b]

INFN Sezione di Firenze [a], Università di Firenze [b], Firenze, Italy
G. Barbagli[a], V. Ciulli[a,b], C. Civinini[a], R. D'Alessandro[a,b], E. Focardi[a,b], S. Gonzi[a,b], V. Gori[a,b], P. Lenzi[a,b], M. Meschini[a], S. Paoletti[a], G. Sguazzoni[a], A. Tropiano[a,b], L. Viliani[a,b]

INFN Laboratori Nazionali di Frascati, Frascati, Italy
L. Benussi, S. Bianco, F. Fabbri, D. Piccolo, F. Primavera

INFN Sezione di Genova [a], Università di Genova [b], Genova, Italy
V. Calvelli[a,b], F. Ferro[a], M. Lo Vetere[a,b], M.R. Monge[a,b], E. Robutti[a], S. Tosi[a,b]

INFN Sezione di Milano-Bicocca [a], Università di Milano-Bicocca [b], Milano, Italy
L. Brianza, M.E. Dinardo[a,b], S. Fiorendi[a,b], S. Gennai[a], R. Gerosa[a,b], A. Ghezzi[a,b], P. Govoni[a,b], S. Malvezzi[a], R.A. Manzoni[a,b], B. Marzocchi[a,b,2], D. Menasce[a], L. Moroni[a], M. Paganoni[a,b], D. Pedrini[a], S. Ragazzi[a,b], N. Redaelli[a], T. Tabarelli de Fatis[a,b]

INFN Sezione di Napoli [a], **Università di Napoli 'Federico II'** [b], **Napoli, Italy, Università della Basilicata** [c], **Potenza, Italy, Università G. Marconi** [d], **Roma, Italy**

S. Buontempo[a], N. Cavallo[a,c], S. Di Guida[a,d,2], M. Esposito[a,b], F. Fabozzi[a,c], A.O.M. Iorio[a,b], G. Lanza[a], L. Lista[a], S. Meola[a,d,2], M. Merola[a], P. Paolucci[a,2], C. Sciacca[a,b], F. Thyssen

INFN Sezione di Padova [a], **Università di Padova** [b], **Padova, Italy, Università di Trento** [c], **Trento, Italy**

P. Azzi[a,2], N. Bacchetta[a], L. Benato[a,b], D. Bisello[a,b], A. Boletti[a,b], R. Carlin[a,b], P. Checchia[a], M. Dall'Osso[a,b,2], T. Dorigo[a], F. Gasparini[a,b], U. Gasparini[a,b], F. Gonella[a], A. Gozzelino[a], M. Gulmini[a,31], K. Kanishchev[a,c], S. Lacaprara[a], M. Margoni[a,b], A.T. Meneguzzo[a,b], F. Montecassiano[a], J. Pazzini[a,b], N. Pozzobon[a,b], P. Ronchese[a,b], F. Simonetto[a,b], E. Torassa[a], M. Tosi[a,b], M. Zanetti, P. Zotto[a,b], A. Zucchetta[a,b,2], G. Zumerle[a,b]

INFN Sezione di Pavia [a], **Università di Pavia** [b], **Pavia, Italy**

A. Braghieri[a], A. Magnani[a], P. Montagna[a,b], S.P. Ratti[a,b], V. Re[a], C. Riccardi[a,b], P. Salvini[a], I. Vai[a], P. Vitulo[a,b]

INFN Sezione di Perugia [a], **Università di Perugia** [b], **Perugia, Italy**

L. Alunni Solestizi[a,b], M. Biasini[a,b], G.M. Bilei[a], D. Ciangottini[a,b,2], L. Fanò[a,b], P. Lariccia[a,b], G. Mantovani[a,b], M. Menichelli[a], A. Saha[a], A. Santocchia[a,b], A. Spiezia[a,b]

INFN Sezione di Pisa [a], **Università di Pisa** [b], **Scuola Normale Superiore di Pisa** [c], **Pisa, Italy**

K. Androsov[a,32], P. Azzurri[a], G. Bagliesi[a], J. Bernardini[a], T. Boccali[a], G. Broccolo[a,c], R. Castaldi[a], M.A. Ciocci[a,32], R. Dell'Orso[a], S. Donato[a,c,2], G. Fedi, L. Foà[a,c†], A. Giassi[a], M.T. Grippo[a,32], F. Ligabue[a,c], T. Lomtadze[a], L. Martini[a,b], A. Messineo[a,b], F. Palla[a], A. Rizzi[a,b], A. Savoy-Navarro[a,33], A.T. Serban[a], P. Spagnolo[a], P. Squillacioti[a,32], R. Tenchini[a], G. Tonelli[a,b], A. Venturi[a], P.G. Verdini[a]

INFN Sezione di Roma [a], **Università di Roma** [b], **Roma, Italy**

L. Barone[a,b], F. Cavallari[a], G. D'imperio[a,b,2], D. Del Re[a,b], M. Diemoz[a], S. Gelli[a,b], C. Jorda[a], E. Longo[a,b], F. Margaroli[a,b], P. Meridiani[a], G. Organtini[a,b], R. Paramatti[a], F. Preiato[a,b], S. Rahatlou[a,b], C. Rovelli[a], F. Santanastasio[a,b], P. Traczyk[a,b,2]

INFN Sezione di Torino [a], **Università di Torino** [b], **Torino, Italy, Università del Piemonte Orientale** [c], **Novara, Italy**

N. Amapane[a,b], R. Arcidiacono[a,c,2], S. Argiro[a,b], M. Arneodo[a,c], R. Bellan[a,b], C. Biino[a], N. Cartiglia[a], M. Costa[a,b], R. Covarelli[a,b], A. Degano[a,b], N. Demaria[a], L. Finco[a,b,2], B. Kiani[a,b], C. Mariotti[a], S. Maselli[a], E. Migliore[a,b], V. Monaco[a,b], E. Monteil[a,b], M. Musich[a], M.M. Obertino[a,b], L. Pacher[a,b], N. Pastrone[a], M. Pelliccioni[a], G.L. Pinna Angioni[a,b], F. Ravera[a,b], A. Romero[a,b], M. Ruspa[a,c], R. Sacchi[a,b], A. Solano[a,b], A. Staiano[a], U. Tamponi[a]

INFN Sezione di Trieste ^{a}, Università di Trieste ^{b}, Trieste, Italy

S. Belforte[a], V. Candelise[a,b,2], M. Casarsa[a], F. Cossutti[a], G. Della Ricca[a,b], B. Gobbo[a], C. La Licata[a,b], M. Marone[a,b], A. Schizzi[a,b], A. Zanetti[a]

Kangwon National University, Chunchon, Korea

A. Kropivnitskaya, S.K. Nam

Kyungpook National University, Daegu, Korea

D.H. Kim, G.N. Kim, M.S. Kim, D.J. Kong, S. Lee, Y.D. Oh, A. Sakharov, D.C. Son

Chonbuk National University, Jeonju, Korea

J.A. Brochero Cifuentes, H. Kim, T.J. Kim

Chonnam National University, Institute for Universe and Elementary Particles, Kwangju, Korea

S. Song

Korea University, Seoul, Korea

S. Choi, Y. Go, D. Gyun, B. Hong, M. Jo, H. Kim, Y. Kim, B. Lee, K. Lee, K.S. Lee, S. Lee, S.K. Park, Y. Roh

Seoul National University, Seoul, Korea

H.D. Yoo

University of Seoul, Seoul, Korea

M. Choi, H. Kim, J.H. Kim, J.S.H. Lee, I.C. Park, G. Ryu, M.S. Ryu

Sungkyunkwan University, Suwon, Korea

Y. Choi, J. Goh, D. Kim, E. Kwon, J. Lee, I. Yu

Vilnius University, Vilnius, Lithuania

A. Juodagalvis, J. Vaitkus

National Centre for Particle Physics, Universiti Malaya, Kuala Lumpur, Malaysia

I. Ahmed, Z.A. Ibrahim, J.R. Komaragiri, M.A.B. Md Ali[34], F. Mohamad Idris[35], W.A.T. Wan Abdullah, M.N. Yusli

Centro de Investigacion y de Estudios Avanzados del IPN, Mexico City, Mexico

E. Casimiro Linares, H. Castilla-Valdez, E. De La Cruz-Burelo, I. Heredia-De La Cruz[36], A. Hernandez-Almada, R. Lopez-Fernandez, A. Sanchez-Hernandez

Universidad Iberoamericana, Mexico City, Mexico

S. Carrillo Moreno, F. Vazquez Valencia

Benemerita Universidad Autonoma de Puebla, Puebla, Mexico

I. Pedraza, H.A. Salazar Ibarguen

Universidad Autónoma de San Luis Potosí, San Luis Potosí, Mexico

A. Morelos Pineda

University of Auckland, Auckland, New Zealand

D. Krofcheck

University of Canterbury, Christchurch, New Zealand

P.H. Butler

National Centre for Physics, Quaid-I-Azam University, Islamabad, Pakistan

A. Ahmad, M. Ahmad, Q. Hassan, H.R. Hoorani, W.A. Khan, T. Khurshid, M. Shoaib

National Centre for Nuclear Research, Swierk, Poland

H. Bialkowska, M. Bluj, B. Boimska, T. Frueboes, M. Górski, M. Kazana, K. Nawrocki, K. Romanowska-Rybinska, M. Szleper, P. Zalewski

Institute of Experimental Physics, Faculty of Physics, University of Warsaw, Warsaw, Poland

G. Brona, K. Bunkowski, A. Byszuk[37], K. Doroba, A. Kalinowski, M. Konecki, J. Krolikowski, M. Misiura, M. Olszewski, M. Walczak

Laboratório de Instrumentação e Física Experimental de Partículas, Lisboa, Portugal

P. Bargassa, C. Beirão Da Cruz E Silva, A. Di Francesco, P. Faccioli, P.G. Ferreira Parracho, M. Gallinaro, N. Leonardo, L. Lloret Iglesias, F. Nguyen, J. Rodrigues Antunes, J. Seixas, O. Toldaiev, D. Vadruccio, J. Varela, P. Vischia

Joint Institute for Nuclear Research, Dubna, Russia

S. Afanasiev, P. Bunin, M. Gavrilenko, I. Golutvin, I. Gorbunov, A. Kamenev, V. Karjavin, V. Konoplyanikov, A. Lanev, A. Malakhov, V. Matveev[38], P. Moisenz, V. Palichik, V. Perelygin, S. Shmatov, S. Shulha, N. Skatchkov, V. Smirnov, A. Zarubin

Petersburg Nuclear Physics Institute, Gatchina (St. Petersburg), Russia

V. Golovtsov, Y. Ivanov, V. Kim[39], E. Kuznetsova, P. Levchenko, V. Murzin, V. Oreshkin, I. Smirnov, V. Sulimov, L. Uvarov, S. Vavilov, A. Vorobyev

Institute for Nuclear Research, Moscow, Russia

Yu. Andreev, A. Dermenev, S. Gninenko, N. Golubev, A. Karneyeu, M. Kirsanov, N. Krasnikov, A. Pashenkov, D. Tlisov, A. Toropin

Institute for Theoretical and Experimental Physics, Moscow, Russia

V. Epshteyn, V. Gavrilov, N. Lychkovskaya, V. Popov, I. Pozdnyakov, G. Safronov, A. Spiridonov, E. Vlasov, A. Zhokin

National Research Nuclear University 'Moscow Engineering Physics Institute' (MEPhI), Moscow, Russia

A. Bylinkin

P.N. Lebedev Physical Institute, Moscow, Russia

V. Andreev, M. Azarkin[40], I. Dremin[40], M. Kirakosyan, A. Leonidov[40], G. Mesyats, S.V. Rusakov

Skobeltsyn Institute of Nuclear Physics, Lomonosov Moscow State University, Moscow, Russia

A. Baskakov, A. Belyaev, E. Boos, M. Dubinin[41], L. Dudko, A. Ershov, A. Gribushin, V. Klyukhin, O. Kodolova, I. Lokhtin, I. Myagkov, S. Obraztsov, S. Petrushanko, V. Savrin, A. Snigirev

State Research Center of Russian Federation, Institute for High Energy Physics, Protvino, Russia

I. Azhgirey, I. Bayshev, S. Bitioukov, V. Kachanov, A. Kalinin, D. Konstantinov, V. Krychkine, V. Petrov, R. Ryutin, A. Sobol, L. Tourtchanovitch, S. Troshin, N. Tyurin, A. Uzunian, A. Volkov

University of Belgrade, Faculty of Physics and Vinca Institute of Nuclear Sciences, Belgrade, Serbia

P. Adzic[42], J. Milosevic, V. Rekovic

Centro de Investigaciones Energéticas Medioambientales y Tecnológicas (CIEMAT), Madrid, Spain

J. Alcaraz Maestre, E. Calvo, M. Cerrada, M. Chamizo Llatas, N. Colino, B. De La Cruz, A. Delgado Peris, D. Domínguez Vázquez, A. Escalante Del Valle, C. Fernandez Bedoya, J.P. Fernández Ramos, J. Flix, M.C. Fouz, P. Garcia-Abia, O. Gonzalez Lopez, S. Goy Lopez, J.M. Hernandez, M.I. Josa, E. Navarro De Martino, A. Pérez-Calero Yzquierdo, J. Puerta Pelayo, A. Quintario Olmeda, I. Redondo, L. Romero, J. Santaolalla, M.S. Soares

Universidad Autónoma de Madrid, Madrid, Spain

C. Albajar, J.F. de Trocóniz, M. Missiroli, D. Moran

Universidad de Oviedo, Oviedo, Spain

J. Cuevas, J. Fernandez Menendez, S. Folgueras, I. Gonzalez Caballero, E. Palencia Cortezon, J.M. Vizan Garcia

Instituto de Física de Cantabria (IFCA), CSIC-Universidad de Cantabria, Santander, Spain

I.J. Cabrillo, A. Calderon, J.R. Castiñeiras De Saa, P. De Castro Manzano, J. Duarte Campderros, M. Fernandez, J. Garcia-Ferrero, G. Gomez, A. Lopez Virto, J. Marco, R. Marco, C. Martinez Rivero, F. Matorras, F.J. Munoz Sanchez, J. Piedra Gomez, T. Rodrigo, A.Y. Rodríguez-Marrero, A. Ruiz-Jimeno, L. Scodellaro, I. Vila, R. Vilar Cortabitarte

CERN, European Organization for Nuclear Research, Geneva, Switzerland

D. Abbaneo, E. Auffray, G. Auzinger, M. Bachtis, P. Baillon, A.H. Ball, D. Barney, A. Benaglia, J. Bendavid, L. Benhabib, J.F. Benitez, G.M. Berruti, P. Bloch, A. Bocci, A. Bonato, C. Botta, H. Breuker, T. Camporesi, R. Castello, G. Cerminara, M. D'Alfonso, D. d'Enterria, A. Dabrowski, V. Daponte, A. David, M. De Gruttola, F. De Guio, A. De Roeck, S. De Visscher, E. Di Marco, M. Dobson, M. Dordevic, B. Dorney, T. du Pree, M. Dünser, N. Dupont, A. Elliott-Peisert, G. Franzoni, W. Funk, D. Gigi, K. Gill, D. Giordano, M. Girone, F. Glege, R. Guida, S. Gundacker, M. Guthoff, J. Hammer,

P. Harris, J. Hegeman, V. Innocente, P. Janot, H. Kirschenmann, M.J. Kortelainen, K. Kousouris, K. Krajczar, P. Lecoq, C. Lourenço, M.T. Lucchini, N. Magini, L. Malgeri, M. Mannelli, A. Martelli, L. Masetti, F. Meijers, S. Mersi, E. Meschi, F. Moortgat, S. Morovic, M. Mulders, M.V. Nemallapudi, H. Neugebauer, S. Orfanelli[43], L. Orsini, L. Pape, E. Perez, M. Peruzzi, A. Petrilli, G. Petrucciani, A. Pfeiffer, D. Piparo, A. Racz, G. Rolandi[44], M. Rovere, M. Ruan, H. Sakulin, C. Schäfer, C. Schwick, A. Sharma, P. Silva, M. Simon, P. Sphicas[45], D. Spiga, J. Steggemann, B. Stieger, M. Stoye, Y. Takahashi, D. Treille, A. Triossi, A. Tsirou, G.I. Veres[22], N. Wardle, H.K. Wöhri, A. Zagozdzinska[37], W.D. Zeuner

Paul Scherrer Institut, Villigen, Switzerland

W. Bertl, K. Deiters, W. Erdmann, R. Horisberger, Q. Ingram, H.C. Kaestli, D. Kotlinski, U. Langenegger, D. Renker, T. Rohe

Institute for Particle Physics, ETH Zurich, Zurich, Switzerland

F. Bachmair, L. Bäni, L. Bianchini, M.A. Buchmann, B. Casal, G. Dissertori, M. Dittmar, M. Donegà, P. Eller, C. Grab, C. Heidegger, D. Hits, J. Hoss, G. Kasieczka, W. Lustermann, B. Mangano, M. Marionneau, P. Martinez Ruiz del Arbol, M. Masciovecchio, D. Meister, F. Micheli, P. Musella, F. Nessi-Tedaldi, F. Pandolfi, J. Pata, F. Pauss, L. Perrozzi, M. Quittnat, M. Rossini, A. Starodumov[46], M. Takahashi, V.R. Tavolaro, K. Theofilatos, R. Wallny

Universität Zürich, Zurich, Switzerland

T.K. Aarrestad, C. Amsler[47], L. Caminada, M.F. Canelli, V. Chiochia, A. De Cosa, C. Galloni, A. Hinzmann, T. Hreus, B. Kilminster, C. Lange, J. Ngadiuba, D. Pinna, P. Robmann, F.J. Ronga, D. Salerno, Y. Yang

National Central University, Chung-Li, Taiwan

M. Cardaci, K.H. Chen, T.H. Doan, Sh. Jain, R. Khurana, M. Konyushikhin, C.M. Kuo, W. Lin, Y.J. Lu, S.S. Yu

National Taiwan University (NTU), Taipei, Taiwan

Arun Kumar, R. Bartek, P. Chang, Y.H. Chang, Y.W. Chang, Y. Chao, K.F. Chen, P.H. Chen, C. Dietz, F. Fiori, U. Grundler, W.-S. Hou, Y. Hsiung, Y.F. Liu, R.-S. Lu, M. Miñano Moya, E. Petrakou, J.f. Tsai, Y.M. Tzeng

Chulalongkorn University, Faculty of Science, Department of Physics, Bangkok, Thailand

B. Asavapibhop, K. Kovitanggoon, G. Singh, N. Srimanobhas, N. Suwonjandee

Cukurova University, Adana, Turkey

A. Adiguzel, S. Cerci[48], Z.S. Demiroglu, C. Dozen, I. Dumanoglu, S. Girgis, G. Gokbulut, Y. Guler, E. Gurpinar, I. Hos, E.E. Kangal[49], A. Kayis Topaksu, G. Onengut[50], K. Ozdemir[51], S. Ozturk[52], B. Tali[48], H. Topakli[52], M. Vergili, C. Zorbilmez

Middle East Technical University, Physics Department, Ankara, Turkey

I.V. Akin, B. Bilin, S. Bilmis, B. Isildak[53], G. Karapinar[54], M. Yalvac, M. Zeyrek

Bogazici University, Istanbul, Turkey

E.A. Albayrak[55], E. Gülmez, M. Kaya[56], O. Kaya[57], T. Yetkin[58]

Istanbul Technical University, Istanbul, Turkey

K. Cankocak, S. Sen[59], F.I. Vardarlı

Institute for Scintillation Materials of National Academy of Science of Ukraine, Kharkov, Ukraine

B. Grynyov

National Scientific Center, Kharkov Institute of Physics and Technology, Kharkov, Ukraine

L. Levchuk, P. Sorokin

University of Bristol, Bristol, United Kingdom

R. Aggleton, F. Ball, L. Beck, J.J. Brooke, E. Clement, D. Cussans, H. Flacher, J. Goldstein, M. Grimes, G.P. Heath, H.F. Heath, J. Jacob, L. Kreczko, C. Lucas, Z. Meng, D.M. Newbold[60], S. Paramesvaran, A. Poll, T. Sakuma, S. Seif El Nasr-storey, S. Senkin, D. Smith, V.J. Smith

Rutherford Appleton Laboratory, Didcot, United Kingdom

D. Barducci, K.W. Bell, A. Belyaev[61], C. Brew, R.M. Brown, D. Cieri, D.J.A. Cockerill, J.A. Coughlan, K. Harder, S. Harper, S. Moretti, E. Olaiya, D. Petyt, C.H. Shepherd-Themistocleous, A. Thea, I.R. Tomalin, T. Williams, W.J. Womersley, S.D. Worm

Imperial College, London, United Kingdom

M. Baber, R. Bainbridge, O. Buchmuller, A. Bundock, D. Burton, S. Casasso, M. Citron, D. Colling, L. Corpe, N. Cripps, P. Dauncey, G. Davies, A. De Wit, M. Della Negra, P. Dunne, A. Elwood, W. Ferguson, J. Fulcher, D. Futyan, G. Hall, G. Iles, M. Kenzie, R. Lane, R. Lucas[60], L. Lyons, A.-M. Magnan, S. Malik, J. Nash, A. Nikitenko[46], J. Pela, M. Pesaresi, K. Petridis, D.M. Raymond, A. Richards, A. Rose, C. Seez, A. Tapper, K. Uchida, M. Vazquez Acosta[62], T. Virdee, S.C. Zenz

Brunel University, Uxbridge, United Kingdom

J.E. Cole, P.R. Hobson, A. Khan, P. Kyberd, D. Leggat, D. Leslie, I.D. Reid, P. Symonds, L. Teodorescu, M. Turner

Baylor University, Waco, U.S.A.

A. Borzou, K. Call, J. Dittmann, K. Hatakeyama, A. Kasmi, H. Liu, N. Pastika

The University of Alabama, Tuscaloosa, U.S.A.

O. Charaf, S.I. Cooper, C. Henderson, P. Rumerio

Boston University, Boston, U.S.A.

A. Avetisyan, T. Bose, C. Fantasia, D. Gastler, P. Lawson, D. Rankin, C. Richardson, J. Rohlf, J. St. John, L. Sulak, D. Zou

Brown University, Providence, U.S.A.

J. Alimena, E. Berry, S. Bhattacharya, D. Cutts, N. Dhingra, A. Ferapontov, A. Garabedian, J. Hakala, U. Heintz, E. Laird, G. Landsberg, Z. Mao, M. Narain, S. Piperov, S. Sagir, T. Sinthuprasith, R. Syarif

University of California, Davis, Davis, U.S.A.

R. Breedon, G. Breto, M. Calderon De La Barca Sanchez, S. Chauhan, M. Chertok, J. Conway, R. Conway, P.T. Cox, R. Erbacher, M. Gardner, W. Ko, R. Lander, M. Mulhearn, D. Pellett, J. Pilot, F. Ricci-Tam, S. Shalhout, J. Smith, M. Squires, D. Stolp, M. Tripathi, S. Wilbur, R. Yohay

University of California, Los Angeles, U.S.A.

R. Cousins, P. Everaerts, C. Farrell, J. Hauser, M. Ignatenko, D. Saltzberg, E. Takasugi, V. Valuev, M. Weber

University of California, Riverside, Riverside, U.S.A.

K. Burt, R. Clare, J. Ellison, J.W. Gary, G. Hanson, J. Heilman, M. Ivova PANEVA, P. Jandir, E. Kennedy, F. Lacroix, O.R. Long, A. Luthra, M. Malberti, M. Olmedo Negrete, A. Shrinivas, H. Wei, S. Wimpenny, B. R. Yates

University of California, San Diego, La Jolla, U.S.A.

J.G. Branson, G.B. Cerati, S. Cittolin, R.T. D'Agnolo, A. Holzner, R. Kelley, D. Klein, J. Letts, I. Macneill, D. Olivito, S. Padhi, M. Pieri, M. Sani, V. Sharma, S. Simon, M. Tadel, A. Vartak, S. Wasserbaech[63], C. Welke, F. Würthwein, A. Yagil, G. Zevi Della Porta

University of California, Santa Barbara, Santa Barbara, U.S.A.

D. Barge, J. Bradmiller-Feld, C. Campagnari, A. Dishaw, V. Dutta, K. Flowers, M. Franco Sevilla, P. Geffert, C. George, F. Golf, L. Gouskos, J. Gran, J. Incandela, C. Justus, N. Mccoll, S.D. Mullin, J. Richman, D. Stuart, I. Suarez, W. To, C. West, J. Yoo

California Institute of Technology, Pasadena, U.S.A.

D. Anderson, A. Apresyan, A. Bornheim, J. Bunn, Y. Chen, J. Duarte, A. Mott, H.B. Newman, C. Pena, M. Pierini, M. Spiropulu, J.R. Vlimant, S. Xie, R.Y. Zhu

Carnegie Mellon University, Pittsburgh, U.S.A.

M.B. Andrews, V. Azzolini, A. Calamba, B. Carlson, T. Ferguson, M. Paulini, J. Russ, M. Sun, H. Vogel, I. Vorobiev

University of Colorado Boulder, Boulder, U.S.A.

J.P. Cumalat, W.T. Ford, A. Gaz, F. Jensen, A. Johnson, M. Krohn, T. Mulholland, U. Nauenberg, K. Stenson, S.R. Wagner

Cornell University, Ithaca, U.S.A.

J. Alexander, A. Chatterjee, J. Chaves, J. Chu, S. Dittmer, N. Eggert, N. Mirman, G. Nicolas Kaufman, J.R. Patterson, A. Rinkevicius, A. Ryd, L. Skinnari, L. Soffi, W. Sun, S.M. Tan, W.D. Teo, J. Thom, J. Thompson, J. Tucker, Y. Weng, P. Wittich

Fermi National Accelerator Laboratory, Batavia, U.S.A.

S. Abdullin, M. Albrow, J. Anderson, G. Apollinari, S. Banerjee, L.A.T. Bauerdick, A. Beretvas, J. Berryhill, P.C. Bhat, G. Bolla, K. Burkett, J.N. Butler, H.W.K. Cheung, F. Chlebana, S. Cihangir, V.D. Elvira, I. Fisk, J. Freeman, E. Gottschalk, L. Gray, D. Green, S. Grünendahl, O. Gutsche, J. Hanlon, D. Hare, R.M. Harris, S. Hasegawa, J. Hirschauer, Z. Hu, S. Jindariani, M. Johnson, U. Joshi, A.W. Jung, B. Klima, B. Kreis, S. Kwan[†], S. Lammel, J. Linacre, D. Lincoln, R. Lipton, T. Liu, R. Lopes De Sá, J. Lykken, K. Maeshima, J.M. Marraffino, V.I. Martinez Outschoorn, S. Maruyama, D. Mason, P. McBride, P. Merkel, K. Mishra, S. Mrenna, S. Nahn, C. Newman-Holmes, V. O'Dell, K. Pedro, O. Prokofyev, G. Rakness, E. Sexton-Kennedy, A. Soha, W.J. Spalding, L. Spiegel, L. Taylor, S. Tkaczyk, N.V. Tran, L. Uplegger, E.W. Vaandering, C. Vernieri, M. Verzocchi, R. Vidal, H.A. Weber, A. Whitbeck, F. Yang

University of Florida, Gainesville, U.S.A.

D. Acosta, P. Avery, P. Bortignon, D. Bourilkov, A. Carnes, M. Carver, D. Curry, S. Das, G.P. Di Giovanni, R.D. Field, I.K. Furic, J. Hugon, J. Konigsberg, A. Korytov, J.F. Low, P. Ma, K. Matchev, H. Mei, P. Milenovic[64], G. Mitselmakher, D. Rank, R. Rossin, L. Shchutska, M. Snowball, D. Sperka, N. Terentyev, L. Thomas, J. Wang, S. Wang, J. Yelton

Florida International University, Miami, U.S.A.

S. Hewamanage, S. Linn, P. Markowitz, G. Martinez, J.L. Rodriguez

Florida State University, Tallahassee, U.S.A.

A. Ackert, J.R. Adams, T. Adams, A. Askew, J. Bochenek, B. Diamond, J. Haas, S. Hagopian, V. Hagopian, K.F. Johnson, A. Khatiwada, H. Prosper, M. Weinberg

Florida Institute of Technology, Melbourne, U.S.A.

M.M. Baarmand, V. Bhopatkar, S. Colafranceschi[65], M. Hohlmann, H. Kalakhety, D. Noonan, T. Roy, F. Yumiceva

University of Illinois at Chicago (UIC), Chicago, U.S.A.

M.R. Adams, L. Apanasevich, D. Berry, R.R. Betts, I. Bucinskaite, R. Cavanaugh, O. Evdokimov, L. Gauthier, C.E. Gerber, D.J. Hofman, P. Kurt, C. O'Brien, I.D. Sandoval Gonzalez, C. Silkworth, P. Turner, N. Varelas, Z. Wu, M. Zakaria

The University of Iowa, Iowa City, U.S.A.

B. Bilki[66], W. Clarida, K. Dilsiz, S. Durgut, R.P. Gandrajula, M. Haytmyradov, V. Khristenko, J.-P. Merlo, H. Mermerkaya[67], A. Mestvirishvili, A. Moeller, J. Nachtman, H. Ogul, Y. Onel, F. Ozok[55], A. Penzo, C. Snyder, P. Tan, E. Tiras, J. Wetzel, K. Yi

Johns Hopkins University, Baltimore, U.S.A.

I. Anderson, B.A. Barnett, B. Blumenfeld, N. Eminizer, D. Fehling, L. Feng, A.V. Gritsan, P. Maksimovic, C. Martin, M. Osherson, J. Roskes, A. Sady, U. Sarica, M. Swartz, M. Xiao, Y. Xin, C. You

The University of Kansas, Lawrence, U.S.A.

P. Baringer, A. Bean, G. Benelli, C. Bruner, R.P. Kenny III, D. Majumder, M. Malek, M. Murray, S. Sanders, R. Stringer, Q. Wang

Kansas State University, Manhattan, U.S.A.

A. Ivanov, K. Kaadze, S. Khalil, M. Makouski, Y. Maravin, A. Mohammadi, L.K. Saini, N. Skhirtladze, S. Toda

Lawrence Livermore National Laboratory, Livermore, U.S.A.

D. Lange, F. Rebassoo, D. Wright

University of Maryland, College Park, U.S.A.

C. Anelli, A. Baden, O. Baron, A. Belloni, B. Calvert, S.C. Eno, C. Ferraioli, J.A. Gomez, N.J. Hadley, S. Jabeen, R.G. Kellogg, T. Kolberg, J. Kunkle, Y. Lu, A.C. Mignerey, Y.H. Shin, A. Skuja, M.B. Tonjes, S.C. Tonwar

Massachusetts Institute of Technology, Cambridge, U.S.A.

A. Apyan, R. Barbieri, A. Baty, K. Bierwagen, S. Brandt, W. Busza, I.A. Cali, Z. Demiragli, L. Di Matteo, G. Gomez Ceballos, M. Goncharov, D. Gulhan, Y. Iiyama, G.M. Innocenti, M. Klute, D. Kovalskyi, Y.S. Lai, Y.-J. Lee, A. Levin, P.D. Luckey, A.C. Marini, C. Mcginn, C. Mironov, X. Niu, C. Paus, D. Ralph, C. Roland, G. Roland, J. Salfeld-Nebgen, G.S.F. Stephans, K. Sumorok, M. Varma, D. Velicanu, J. Veverka, J. Wang, T.W. Wang, B. Wyslouch, M. Yang, V. Zhukova

University of Minnesota, Minneapolis, U.S.A.

B. Dahmes, A. Evans, A. Finkel, A. Gude, P. Hansen, S. Kalafut, S.C. Kao, K. Klapoetke, Y. Kubota, Z. Lesko, J. Mans, S. Nourbakhsh, N. Ruckstuhl, R. Rusack, N. Tambe, J. Turkewitz

University of Mississippi, Oxford, U.S.A.

J.G. Acosta, S. Oliveros

University of Nebraska-Lincoln, Lincoln, U.S.A.

E. Avdeeva, K. Bloom, S. Bose, D.R. Claes, A. Dominguez, C. Fangmeier, R. Gonzalez Suarez, R. Kamalieddin, J. Keller, D. Knowlton, I. Kravchenko, J. Lazo-Flores, F. Meier, J. Monroy, F. Ratnikov, J.E. Siado, G.R. Snow

State University of New York at Buffalo, Buffalo, U.S.A.

M. Alyari, J. Dolen, J. George, A. Godshalk, C. Harrington, I. Iashvili, J. Kaisen, A. Kharchilava, A. Kumar, S. Rappoccio

Northeastern University, Boston, U.S.A.

G. Alverson, E. Barberis, D. Baumgartel, M. Chasco, A. Hortiangtham, A. Massironi, D.M. Morse, D. Nash, T. Orimoto, R. Teixeira De Lima, D. Trocino, R.-J. Wang, D. Wood, J. Zhang

Northwestern University, Evanston, U.S.A.

K.A. Hahn, A. Kubik, N. Mucia, N. Odell, B. Pollack, A. Pozdnyakov, M. Schmitt, S. Stoynev, K. Sung, M. Trovato, M. Velasco

University of Notre Dame, Notre Dame, U.S.A.

A. Brinkerhoff, N. Dev, M. Hildreth, C. Jessop, D.J. Karmgard, N. Kellams, K. Lannon, S. Lynch, N. Marinelli, F. Meng, C. Mueller, Y. Musienko[38], T. Pearson, M. Planer, A. Reinsvold, R. Ruchti, G. Smith, S. Taroni, N. Valls, M. Wayne, M. Wolf, A. Woodard

The Ohio State University, Columbus, U.S.A.

L. Antonelli, J. Brinson, B. Bylsma, L.S. Durkin, S. Flowers, A. Hart, C. Hill, R. Hughes, W. Ji, K. Kotov, T.Y. Ling, B. Liu, W. Luo, D. Puigh, M. Rodenburg, B.L. Winer, H.W. Wulsin

Princeton University, Princeton, U.S.A.

O. Driga, P. Elmer, J. Hardenbrook, P. Hebda, S.A. Koay, P. Lujan, D. Marlow, T. Medvedeva, M. Mooney, J. Olsen, C. Palmer, P. Piroué, X. Quan, H. Saka, D. Stickland, C. Tully, J.S. Werner, A. Zuranski

University of Puerto Rico, Mayaguez, U.S.A.

S. Malik

Purdue University, West Lafayette, U.S.A.

V.E. Barnes, D. Benedetti, D. Bortoletto, L. Gutay, M.K. Jha, M. Jones, K. Jung, D.H. Miller, N. Neumeister, B.C. Radburn-Smith, X. Shi, I. Shipsey, D. Silvers, J. Sun, A. Svyatkovskiy, F. Wang, W. Xie, L. Xu

Purdue University Calumet, Hammond, U.S.A.

N. Parashar, J. Stupak

Rice University, Houston, U.S.A.

A. Adair, B. Akgun, Z. Chen, K.M. Ecklund, F.J.M. Geurts, M. Guilbaud, W. Li, B. Michlin, M. Northup, B.P. Padley, R. Redjimi, J. Roberts, J. Rorie, Z. Tu, J. Zabel

University of Rochester, Rochester, U.S.A.

B. Betchart, A. Bodek, P. de Barbaro, R. Demina, Y. Eshaq, T. Ferbel, M. Galanti, A. Garcia-Bellido, J. Han, A. Harel, O. Hindrichs, A. Khukhunaishvili, G. Petrillo, M. Verzetti

Rutgers, The State University of New Jersey, Piscataway, U.S.A.

S. Arora, A. Barker, J.P. Chou, C. Contreras-Campana, E. Contreras-Campana, D. Duggan, D. Ferencek, Y. Gershtein, R. Gray, E. Halkiadakis, D. Hidas, E. Hughes, S. Kaplan, R. Kunnawalkam Elayavalli, A. Lath, K. Nash, S. Panwalkar, M. Park, S. Salur, S. Schnetzer, D. Sheffield, S. Somalwar, R. Stone, S. Thomas, P. Thomassen, M. Walker

University of Tennessee, Knoxville, U.S.A.

M. Foerster, G. Riley, K. Rose, S. Spanier, A. York

Texas A&M University, College Station, U.S.A.

O. Bouhali[68], A. Castaneda Hernandez[68], M. Dalchenko, M. De Mattia, A. Delgado, S. Dildick, R. Eusebi, W. Flanagan, J. Gilmore, T. Kamon[69], V. Krutelyov, R. Mueller, I. Osipenkov, Y. Pakhotin, R. Patel, A. Perloff, A. Rose, A. Safonov, A. Tatarinov, K.A. Ulmer[2]

Texas Tech University, Lubbock, U.S.A.

N. Akchurin, C. Cowden, J. Damgov, C. Dragoiu, P.R. Dudero, J. Faulkner, S. Kunori, K. Lamichhane, S.W. Lee, T. Libeiro, S. Undleeb, I. Volobouev

Vanderbilt University, Nashville, U.S.A.

E. Appelt, A.G. Delannoy, S. Greene, A. Gurrola, R. Janjam, W. Johns, C. Maguire, Y. Mao, A. Melo, H. Ni, P. Sheldon, B. Snook, S. Tuo, J. Velkovska, Q. Xu

University of Virginia, Charlottesville, U.S.A.

M.W. Arenton, S. Boutle, B. Cox, B. Francis, J. Goodell, R. Hirosky, A. Ledovskoy, H. Li, C. Lin, C. Neu, X. Sun, Y. Wang, E. Wolfe, J. Wood, F. Xia

Wayne State University, Detroit, U.S.A.

C. Clarke, R. Harr, P.E. Karchin, C. Kottachchi Kankanamge Don, P. Lamichhane, J. Sturdy

University of Wisconsin, Madison, U.S.A.

D.A. Belknap, D. Carlsmith, M. Cepeda, A. Christian, S. Dasu, L. Dodd, S. Duric, E. Friis, B. Gomber, M. Grothe, R. Hall-Wilton, M. Herndon, A. Hervé, P. Klabbers, A. Lanaro, A. Levine, K. Long, R. Loveless, A. Mohapatra, I. Ojalvo, T. Perry, G.A. Pierro, G. Polese, T. Ruggles, T. Sarangi, A. Savin, A. Sharma, N. Smith, W.H. Smith, D. Taylor, N. Woods

†: Deceased
1: Also at Vienna University of Technology, Vienna, Austria
2: Also at CERN, European Organization for Nuclear Research, Geneva, Switzerland
3: Also at State Key Laboratory of Nuclear Physics and Technology, Peking University, Beijing, China
4: Also at Institut Pluridisciplinaire Hubert Curien, Université de Strasbourg, Université de Haute Alsace Mulhouse, CNRS/IN2P3, Strasbourg, France
5: Also at National Institute of Chemical Physics and Biophysics, Tallinn, Estonia
6: Also at Skobeltsyn Institute of Nuclear Physics, Lomonosov Moscow State University, Moscow, Russia
7: Also at Universidade Estadual de Campinas, Campinas, Brazil
8: Also at Centre National de la Recherche Scientifique (CNRS) - IN2P3, Paris, France
9: Also at Laboratoire Leprince-Ringuet, Ecole Polytechnique, IN2P3-CNRS, Palaiseau, France
10: Also at Joint Institute for Nuclear Research, Dubna, Russia
11: Also at Helwan University, Cairo, Egypt
12: Now at Zewail City of Science and Technology, Zewail, Egypt
13: Also at British University in Egypt, Cairo, Egypt
14: Now at Ain Shams University, Cairo, Egypt
15: Also at Université de Haute Alsace, Mulhouse, France
16: Also at Tbilisi State University, Tbilisi, Georgia
17: Also at RWTH Aachen University, III. Physikalisches Institut A, Aachen, Germany
18: Also at Indian Institute of Science Education and Research, Bhopal, India
19: Also at University of Hamburg, Hamburg, Germany
20: Also at Brandenburg University of Technology, Cottbus, Germany

21: Also at Institute of Nuclear Research ATOMKI, Debrecen, Hungary

22: Also at Eötvös Loránd University, Budapest, Hungary

23: Also at University of Debrecen, Debrecen, Hungary

24: Also at Wigner Research Centre for Physics, Budapest, Hungary

25: Also at University of Visva-Bharati, Santiniketan, India

26: Now at King Abdulaziz University, Jeddah, Saudi Arabia

27: Also at University of Ruhuna, Matara, Sri Lanka

28: Also at Isfahan University of Technology, Isfahan, Iran

29: Also at University of Tehran, Department of Engineering Science, Tehran, Iran

30: Also at Plasma Physics Research Center, Science and Research Branch, Islamic Azad University, Tehran, Iran

31: Also at Laboratori Nazionali di Legnaro dell'INFN, Legnaro, Italy

32: Also at Università degli Studi di Siena, Siena, Italy

33: Also at Purdue University, West Lafayette, U.S.A.

34: Also at International Islamic University of Malaysia, Kuala Lumpur, Malaysia

35: Also at Malaysian Nuclear Agency, MOSTI, Kajang, Malaysia

36: Also at Consejo Nacional de Ciencia y Tecnología, Mexico city, Mexico

37: Also at Warsaw University of Technology, Institute of Electronic Systems, Warsaw, Poland

38: Also at Institute for Nuclear Research, Moscow, Russia

39: Also at St. Petersburg State Polytechnical University, St. Petersburg, Russia

40: Also at National Research Nuclear University 'Moscow Engineering Physics Institute' (MEPhI), Moscow, Russia

41: Also at California Institute of Technology, Pasadena, U.S.A.

42: Also at Faculty of Physics, University of Belgrade, Belgrade, Serbia

43: Also at National Technical University of Athens, Athens, Greece

44: Also at Scuola Normale e Sezione dell'INFN, Pisa, Italy

45: Also at University of Athens, Athens, Greece

46: Also at Institute for Theoretical and Experimental Physics, Moscow, Russia

47: Also at Albert Einstein Center for Fundamental Physics, Bern, Switzerland

48: Also at Adiyaman University, Adiyaman, Turkey

49: Also at Mersin University, Mersin, Turkey

50: Also at Cag University, Mersin, Turkey

51: Also at Piri Reis University, Istanbul, Turkey

52: Also at Gaziosmanpasa University, Tokat, Turkey

53: Also at Ozyegin University, Istanbul, Turkey

54: Also at Izmir Institute of Technology, Izmir, Turkey

55: Also at Mimar Sinan University, Istanbul, Istanbul, Turkey

56: Also at Marmara University, Istanbul, Turkey

57: Also at Kafkas University, Kars, Turkey

58: Also at Yildiz Technical University, Istanbul, Turkey

59: Also at Hacettepe University, Ankara, Turkey

60: Also at Rutherford Appleton Laboratory, Didcot, United Kingdom

61: Also at School of Physics and Astronomy, University of Southampton, Southampton, United Kingdom

62: Also at Instituto de Astrofísica de Canarias, La Laguna, Spain

63: Also at Utah Valley University, Orem, U.S.A.

64: Also at University of Belgrade, Faculty of Physics and Vinca Institute of Nuclear Sciences, Belgrade, Serbia

65: Also at Facoltà Ingegneria, Università di Roma, Roma, Italy
66: Also at Argonne National Laboratory, Argonne, U.S.A.
67: Also at Erzincan University, Erzincan, Turkey
68: Also at Texas A&M University at Qatar, Doha, Qatar
69: Also at Kyungpook National University, Daegu, Korea